SSRG International Journal of Civil Engineering
ISSN: 2348-8352/ https://doi.org/10.14445/23488352/IJCE-V13I4P117

Volume 13 Issue 4, 275-300, April 2026

Original Article

Evaluation of the Effectiveness of Viscous Fluid in Chevron Brace Arrangement and Tuned Mass for the Control of Structures with Irregularity of Incoming Corners

Jannyna Nataly Ramos Comun[1], Victor Manuel Garay Gora[1], Jose Jheyson Ccanto Luis[1], Manuel Ismael Laurencio Luna[1*]

[1]*Faculty of Civil Engineering, Continental University, 12001, Huancayo, Perú.*

**Corresponding Author : mlaurencio@continental.edu.pe*

Received: 12 January 2026 Revised: 15 February 2026 Accepted: 19 March 2026 Published: 28 April 2026

Abstract - *Peru is located in the Pacific Ring of Fire, prone to earthquakes, particularly in buildings whose construction is defined by quaker irregularities, like such in the geaming of the polygonal L, in which the corners overseeing construction recesses, thereby creating mass torsion of the rigid blocks, creating a torsional rapture increasing primary weaknesses of the buildings framed in the geplants. Under such conditions, the research assesses the VFDs in chevron-braced systems, and the other is a TMD, and this is framed within the 10-20 story Ls bonoment of the buildings Senator E034- 150ft. The responses are modelled with ETABS, and the Structures Ease has confirmed that indeed there is viscosity, but the total effort is aimed at generating a further 59.93%, controlling the 58.43% acceleration, 56.31% control of drifting, and 48.14% control. To achieve this, the 10 to 15-storey buildings (10-15) should be able to increase viscosity. In contrast, the TMD was more efficient in tall buildings (18–20 storeys), with reductions in displacement of up to 60.27%, drifts of 49.21%, accelerations of 32.27%, and basal shear of 59.92%, due to its resonant energy absorption when the tuning frequency coincides with that of the predominant structural mode. In conclusion, the Chevron Brace is more stable and versatile in compact buildings, while the TMD is more effective in slender structures. Both systems complement each other by controlling accelerations and displacements, keeping the structural response within the elastic range, and improving the seismic safety of buildings with geometric irregularities.*

Keywords - *Chevron brace, Tuned mass, Irregularity of inward corners, Collapse, Drifts.*

1. Introduction

Peru, located in the Pacific Ring of Fire, is one of the countries most exposed to seismic activity worldwide, facing frequent and large-magnitude earthquakes that threaten both the safety of its infrastructure and the lives of its population. Faced with this situation, the 2023 Seismic Map of the Instituto Geofísico del Perú (IGP) [1] reveals that much of the national territory is located in areas of high seismic hazard, especially the central and southern coast, where events exceeding 8.0 Mw have been recorded. One of the most representative examples occurred in the southern region: the 2007 Pisco earthquake, with a magnitude of 7.9 Mw, considered one of the most devastating in the country's recent history, left more than 500 dead and severely damaged more than 75000 homes [2]. This disaster highlighted the high vulnerability of buildings, particularly mid-rise buildings (between 10 and 20 storeys), which exhibit complex dynamic behavior due to the effects of vibration amplification, significantly increasing the risk of severe structural damage or even collapse during an earthquake [3]. Despite the existence of earthquake-resistant regulations such as Technical Standard E.030 on Earthquake-Resistant Design, many buildings in the country remain vulnerable, especially those constructed with geometric irregularities that affect their seismic performance. In particular, structures with recessed corners have an irregular distribution of mass and stiffness, which generates eccentricity between the center of mass and the center of stiffness, resulting in torsion and stress concentration in vulnerable areas [4]. This type of geometric irregularity has been the subject of numerous studies, which have shown that it can significantly increase seismic demand compared to buildings with more regular geometries [5]. In order to mitigate the negative effects of these structural problems, various technological solutions have been proposed, including Tuned Mass Dampers (TMDs) and Viscous Fluid Dissipators (VFDs) [6, 7]. Both systems have proven effective in reducing seismic response in buildings, with TMDs being particularly

effective in attenuating high-frequency oscillations, while DFVs contribute to improving structural stability by dissipating seismic energy through fluid viscosity [8, 9] However, most existing studies have evaluated these systems independently or in structures with regular configurations, without addressing their comparative performance in buildings with plan irregularities such as re-entrant corners.

This reveals a critical research gap: the absence of comparative evaluations of TMDs and VFDs in mid-rise buildings with geometric irregularities under seismic conditions representative of the Peruvian context. This limitation restricts the ability to select efficient passive control strategies for structurally irregular buildings, which are common in urban environments.

In response to this gap, this study aims to evaluate and compare the effectiveness of viscous fluid dampers (VFDs), arranged in a Chevron Brace configuration, and tuned mass dampers (TMDs) in controlling the seismic response of buildings with re-entrant corner irregularities. The analysis focuses on mid-rise buildings ranging from 10 to 20 storeys, with an L-shaped plan area of 1,225 m² and a built-up area of 1,125 m². The structures are modeled using ETABS software to assess passive control strategies capable of mitigating the adverse effects of geometric irregularity and improving structural performance under high seismic demand.

The novelty of this research lies not only in the direct comparison between TMDs and VFDs in irregular configurations, but also in their application within a structural model representative of the Peruvian seismic context, providing practical criteria for the design and optimization of passive control systems in mid-rise irregular buildings.

2. Literature Review

2.1. Seismic Vulnerability of Buildings in Peru

Over the years, major earthquakes in Peru have demonstrated the high vulnerability of buildings to severe seismic events, causing catastrophic consequences in terms of both human and material losses. Figure 1 presents some of the most representative earthquakes recorded in the country. In item A, the 2007 Pisco earthquake, with a magnitude of 7.9 Mw, caused more than 500 deaths and affected more than 75,000 homes [10]. Item B) In 2001, the Arequipa earthquake with a magnitude of 8.4 Mw resulted in more than 100 deaths and thousands of damaged homes [11]. Item C) In 2005, the earthquake in the San Martín region with a magnitude of 7.5 Mw caused serious damage to homes and other buildings [12]. Item D) The Lima earthquake in 1974, measuring 7.7 Mw, brought to the forefront the construction weaknesses in the buildings within the city [13]. Taken together, these events reveal the persistent seismic risk in Peru and the urgent need to improve the structural performance of buildings exposed to strong ground motion.

Item a. Pisco

Item b. Arequipa

Item c. San Martín

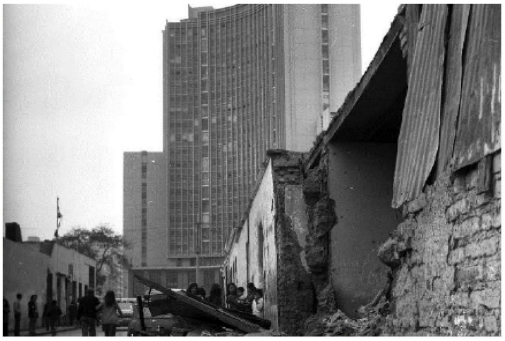

Item d. Lima

Fig. 1 Earthquakes in Peru

2.2. Seismic Effects of Re-Entrant Corner Irregularities

Research conducted after major earthquakes has confirmed that structures with irregular geometries tend to experience greater damage than geometrically regular buildings [14]. Among plan irregularities, re-entrant corners are particularly critical because they generate abrupt changes in stiffness and mass distribution, leading to torsional effects, stress concentration, and uneven lateral displacement demands.

Figure 2 shows examples of buildings with re-entrant corner irregularities in different countries. In item (a), corresponding to Venezuela, a building with pronounced inward corners is observed, which may compromise the uniform distribution of seismic forces [15]. In item (b), in Alaska, a structural configuration with multiple acute re-entrant corners is identified, creating potentially vulnerable zones under seismic loading [4]. Finally, in item (c), corresponding to Peru, pronounced inward corners are also evident, which may adversely affect structural performance [16]. These examples illustrate that this type of irregularity is not limited to a single regional context, but rather represents a widespread structural configuration associated with higher seismic demand.

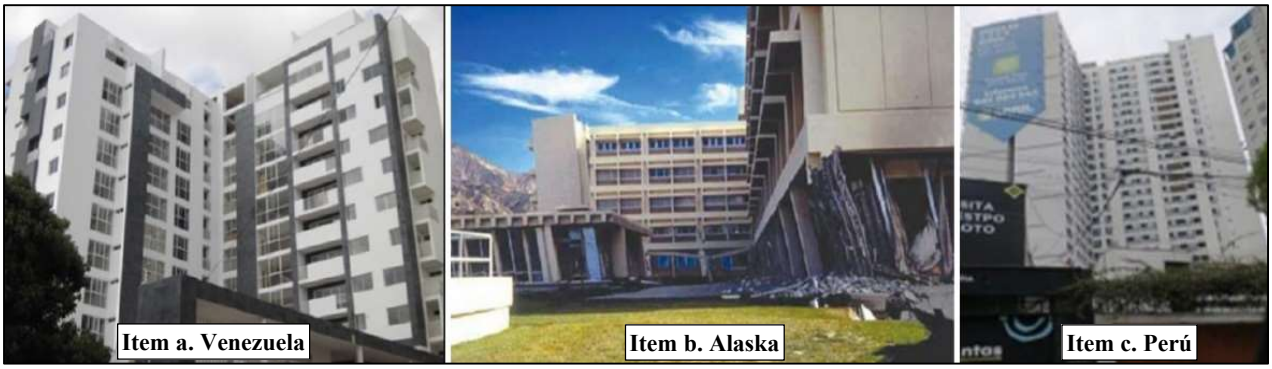

Fig. 1 Buildings with irregular recessed corners in different countries

Several studies have investigated the seismic behavior of buildings with re-entrant corner irregularities. In the Kingdom of Saudi Arabia, the seismic behaviour of L-shaped buildings with re-entrant corners was analysed, comparing them with a symmetrical nine-story model. Six additional models with different degrees of irregularity in plan were developed, and variables such as inter-story drift, shear force, overturning moment, and torsion at the base were evaluated. The results showed that irregular buildings have higher stress concentrations and more pronounced lateral-torsional coupling, which increases their seismic vulnerability. In addition, there was a significant increase in shear forces in the vertical elements located at the periphery, compared to regular buildings [4].

In Italy, the optimal location of viscous dampers was evaluated to control torsional response in buildings with asymmetrical floor plans. Models were analysed using modal techniques in state space, highlighting how the distribution of damping influences dynamic behaviour.

Design criteria were set according to the relationships governing maximum edge displacement to seismic excitation in the obtained transfer functions, and parametric assessments were carried out within the bounds of practical limitations. Results demonstrated through numerical simulation comparisons with synthetic and real earthquakes validated that effective placement of dampers enhances control of torsion and reduction of drifts significantly [17].

In Nepal, the seismic performance of L-shaped corner recess R.C. buildings was studied and cross-compared with that of a regular building. Six models were examined with respect to static equivalence and response spectrum analysis, with different seismic arrival angles. Results indicate that irregular buildings have a greater displacement, drift, and torsion, even though the most critical displacement/ torsion was recorded with a 135-degree angle. The study also found that the fundamental period predicted by the code was lower than that obtained through the finite element method, suggesting that conventional design provisions may not adequately represent the dynamic behavior of this type of structure [18].

The seismic behavior of nine story buildings with moment resistant frames was assessed, concentrating on L-shaped irregularities with re-entrant corners, as well as their peculiarities in Egypt. Using ETABS, six models were examined with the Equivalent Static Load and Response Spectrum techniques, analyzing the drift of the storeys, shear force, overturning moment as well as the axial torsion on the building's height. The results of the comparative study revealed that structures with high irregularities were more vulnerable to seismic activities, in contrast to the regular models, considering the shear and torsional forces perpendicular to the seismic input. Furthermore, the study verified that the code-based equation used to estimate the fundamental period does not adequately account for torsional modes, which is highly relevant for the seismic assessment of irregular structures [19].

Passive control systems have emerged as an effective strategy for improving seismic performance. Among them, Tuned Mass Dampers (TMDs) reduce vibratory response through an auxiliary tuned mass, whereas Viscous Fluid Dampers (VFDs) dissipate seismic energy through fluid viscosity, reducing drifts, accelerations, and internal forces.

The relevance of these systems for irregular buildings has also been explored in previous research. The Italian study discussed above demonstrated that the effectiveness of viscous dampers in asymmetric-plan buildings depends not only on the presence of the device, but also on its distribution within the structural layout [17]. This finding is particularly important because it suggests that the efficiency of passive control systems is strongly influenced by the interaction between the control mechanism and the irregular dynamic response of the structure.

Despite these advances, the literature still presents an important limitation. Most previous studies have either focused on the seismic vulnerability of buildings with re-entrant corner irregularities or analyzed the isolated performance of passive control systems, without conducting direct comparisons between different control strategies in the same type of irregular mid-rise structure. Moreover, few studies have addressed this problem under conditions representative of the Peruvian seismic context. Therefore, the existing literature does not yet provide sufficient evidence to determine which passive control strategy is more effective for reducing the seismic response of mid-rise buildings with re-entrant corner irregularities in Peru. This unresolved issue constitutes the main research gap addressed in the present study.

3. Materials and Methods

3.1. Structural Irregularities

Structural irregularities are deficiencies in the design or distribution of elements that affect seismic response and compromise the safety of the structure [20]. One of the most common issues is floor irregularity, which directly influences the seismic behaviour of buildings.

3.2. Structural Irregularities in the Floor Plan

Structural irregularities in the floor plan refer to the uneven or asymmetrical arrangement of structural elements within the floor plan of the building [21]. These irregularities generate undesirable seismic behaviour, such as torsion or stress concentrations, which can affect the stability of the building during an earthquake. Common types of floor plan irregularities are shown in Table 1.

Table 1. Structural irregularities in the floor plan

Irregularity	Description
Torsional irregularity	Occurs when the center of mass does not coincide with the center of rigidity, causing additional rotation in the structure during an earthquake and increasing the risk of damage [22].
Extreme torsional irregularity	Occurs when the difference in stiffness between the horizontal axes is so great that the structure experiences extreme torsion during an earthquake, which can compromise its stability [23].
Indented corners	Occurs when the floor plan has recesses or corners that are not straight, which can cause an uneven distribution of seismic forces, generating stress concentrations in those areas [19].
Diaphragm discontinuity	This refers to the interruption of the diaphragm system (the structure that connects the floors), which prevents seismic forces from being distributed efficiently between the different levels of the building [24].
Non-parallel systems	This occurs when structural elements (such as columns) are not aligned in parallel, which can result in asymmetric behaviour under seismic loads [25].

3.2.1. Irregularity Due to Recessed Corners

Irregularity due to recessed corners is a type of structural irregularity that occurs when the corners of the building's floor plan are recessed, i.e., they have an irregular shape at their vertices [19]. According to Standard E030, "a structure is classified as irregular when it has recessed corners whose dimensions in both directions are greater than 20% of the corresponding total dimension in plan" [26]. Figure 3 shows three representative examples of geometries with inward corners, in which three types of irregularities are identified: an L-shaped notch (simple corner), a double square forming an inverted T, and a deep H-shaped cavity. Each of these configurations has a different degree of impact on structural integrity, as they introduce discontinuities that disrupt the homogeneity of the material and generate stress concentrations at the internal corners. These critical areas can lead to premature failure if not properly addressed during structural design. Dimensions A, B, a, and b allow the proportion and depth of these notches to be quantified, and are key variables for the mechanical analysis and geometric optimisation of the structure.

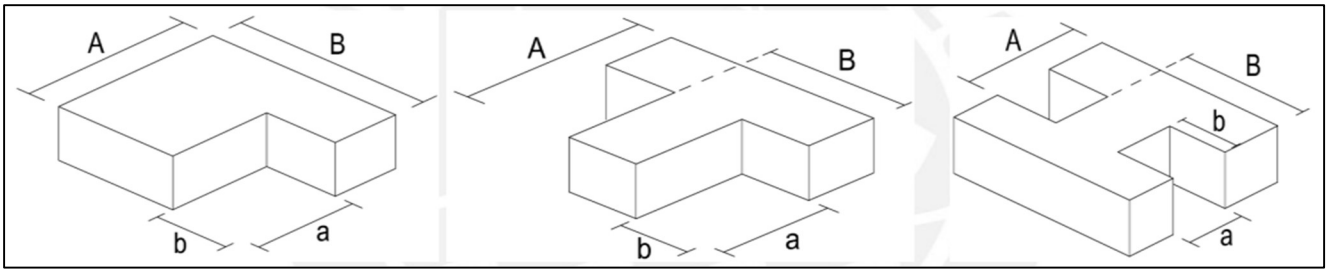

Fig. 3 Types of irregularities due to inward corners

3.3. Viscous Fluid

Viscous fluid is a damping system that mitigates vibrations in structures during an earthquake or any other seismic event [27], and is based on the use of high-viscosity fluids, which, when compressed or displaced through an orifice, dissipate the energy generated by seismic movement, thereby reducing the oscillations of the structure and improving its behaviour in the event of earthquakes. Figure 4 shows the components of the system: the stainless steel piston (1), which acts as the fluid control mechanism; the inert silicone (2), which functions as the viscous fluid that helps dissipate seismic energy; and the seals (3), which ensure the system is watertight and that the fluid circulates correctly.

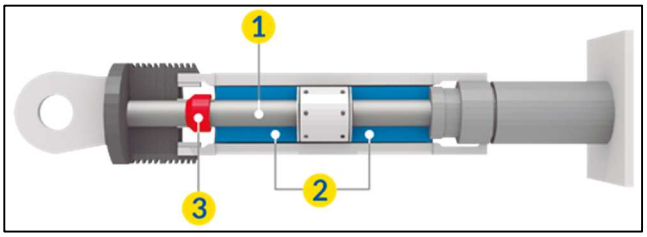

Fig. 4 Viscous fluid shock absorber

3.4. Chevron Brace Arrangement

A Chevron Brace is a structural system that uses a series of inverted V-shaped inclined members [28] (Figure 5) to provide stability to a structure, such as a steel frame, against lateral loads, such as those generated by earthquakes or strong winds [29].

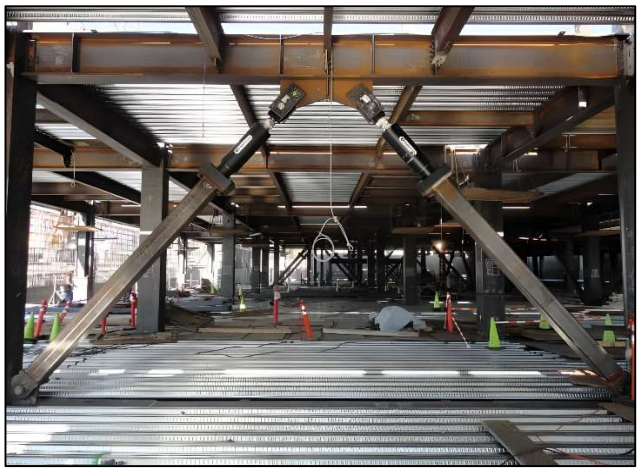

Fig. 5 Viscous fluid damper

To calculate the damping coefficient in the structural system, formula 1 was used, which allows the energy dissipation capacity of the system to be determined by analysing the dynamic properties of the structure:

$$\sum Cj = \frac{\beta h \, x \, 2\pi \, x \, A^{1-\alpha} x \, \omega^{2-\alpha} x \, (\sum_i mi\Phi i^2)}{\lambda(\sum \Phi rj^{1+\alpha} x \, cos^{1+\alpha}\theta j)} \quad (1)$$

Where (j) represents the heat sink and the subscript (i) corresponds to the level number considered in the structure. The term (βh) denotes the overall viscous damping of the structural system, while (mi) indicates the mass associated with level (i).

The parameter (θj) refers to the angle of inclination of the dissipator with respect to the horizontal, and (Φi) expresses the modal displacement at level (i) corresponding to the first mode of vibration. Likewise, (Φrj) represents the relative modal displacement between the two ends of the heat sink in the horizontal direction.

On the other hand, (A) corresponds to the amplitude of the fundamental mode displacement, (ω) symbolises the angular frequency of the system, (λ) is the lambda parameter associated with the mathematical analysis model, and (α) defines the velocity exponent used in the formulation of the non-linear behaviour of the dissipation.

To calculate the angular frequency (ω), formula 2 was used, which establishes a direct relationship between the angular frequency and the natural frequency of the system.

$$\omega = 2 \, x \, \pi \, x \, f \quad (2)$$

Where f is the natural frequency of the system, which is obtained from the oscillation period T, using formula 3.

$$f = \frac{1}{T} \quad (3)$$

The parameter α, known as the velocity exponent, was determined according to the guidelines of FEMA 274 [30], which establishes that its value must be greater than, equal to, or less than 1, as shown in Figure 6. Once the value of α has been obtained, the standard automatically provides the corresponding value for the parameter λ, which was essential for calculating the dynamic behaviour of the structure.

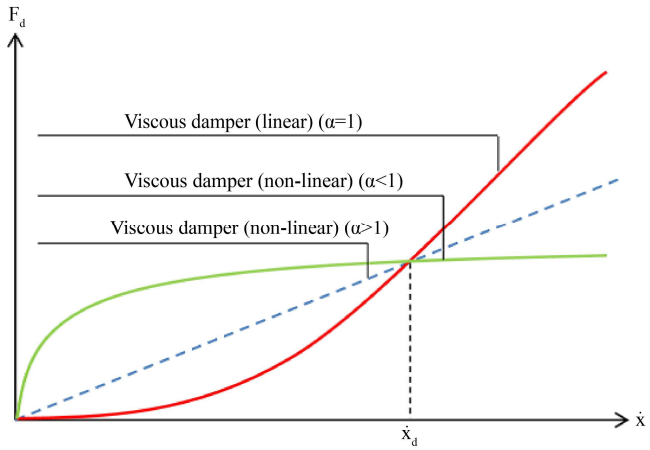

Fig. 6 Speed vs. damping force ratio [31]

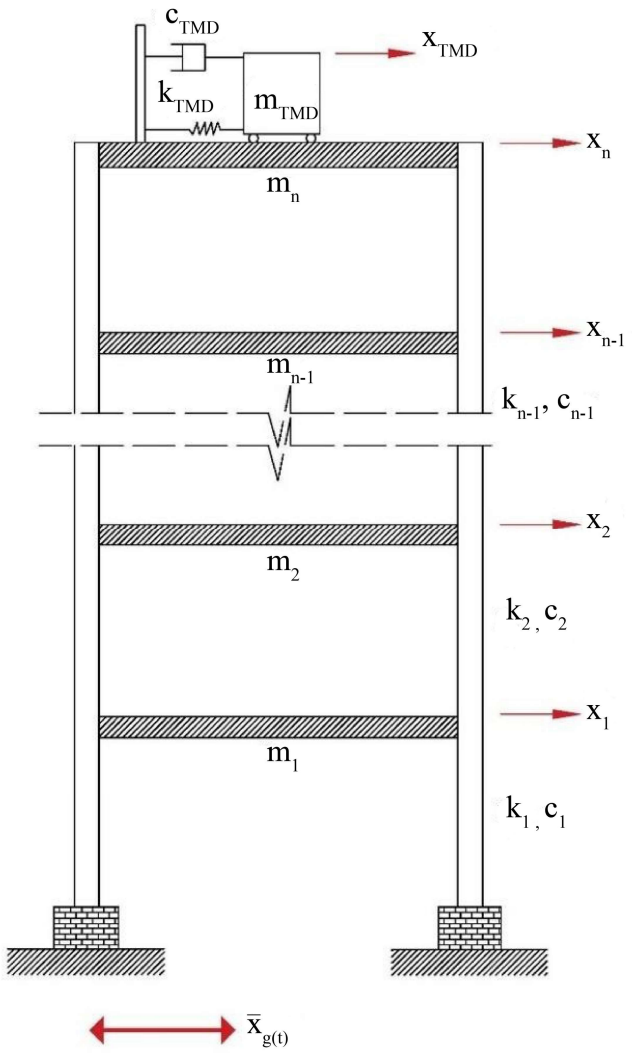

Fig. 7 Tuned mass damper

3.5. Tuned Mass

The tuned mass, usually made of heavy materials such as steel or concrete, consists of a mass located at the top of a building and connected by springs and dampers [32], adjusted so that its natural frequency matches the resonance frequency of the vibrations to be controlled [33]; When the structure vibrates, the mass moves in the opposite direction, generating a damping force that reduces oscillations and improves the stability and safety of tall buildings [34]. Figure 7 shows the tuned mass in a four-story building more clearly. It shows a simplified model of a multi-story building, where the Tuned Mass Damper (TMD) is installed at the top of the structure. This system consists of a tuned mass (KTMD) and a damper with a damping coefficient (CTMD), both of which are connected to the top level of the building. With the respective masses of the floors ($m1$, $m2$, ..., mn), bulk rigidity (k), and viscous damping (c), the dynamic behaviour of the TMD can be modeled to counteract the vibrations induced by ground acceleration $\ddot{g}(t)$. This model enables the participant to study the moving Tuned Mass Dampers (TMD) and the relative displacement of (x1, x2, ..., xn) and all the floors affected by the seismic event.

The primary purpose of alluded equations 4, 5, 6, 7, and 8 is to facilitate the design and customization of a tuned mass damper, and primarily, to give knowledge on how to eliminate the decrease in the mass of a structure, including buildings. The engineering structures of the TMD are calculated using the principle of the mass TMD as highlighted in the first equation, wherein the mass is a function of the weight of the building. The optimal is determined in the second equation, and this is the ultimate energy the TMD is able to spend (controlled) in a vibrating system. The angular frequency of TMD is calculated in the third equation.

This angular frequency is a significant constituent for the TMD to work properly in conjunction with the natural frequency of the building to which the TMD is tuned. The stiffness of the TMD is calculated in the 4th equation. This TMD stiffness is a function of the mass and angular frequency. The 5th equation is used to calculate the damping coefficient. This is the amount of energy absorbed by the TMD from the vibrating system. The prescribed equations can be used to design an efficient TMD, which can be used to shield structures from the adverse impacts of vibrations.

$$m_{TMD} = \%mass * P_{wei} \quad of\ the\ building \tag{4}$$

$$\epsilon_{optimal} = \sqrt{\frac{3*m_{TMD}}{8\,(1+m_{TMD})*(1-0.5*m_{TMD})}} \tag{5}$$

$$W_a = \left(\sqrt{\frac{1-0.5*m_{TMD}}{1+m_{TMD}}}\right) * \frac{2*\pi}{T_{building}} \tag{6}$$

$$k_{TMD} = m_{TMD} * {W_a}^2 \tag{7}$$

$$C_{TMD} = \epsilon_{optimal} * 2 * m_{TMD} * W_a \tag{8}$$

The parameters in the equation are defined as follows: (mTMD) represents the mass of the tuned mass damper (TMD); (ϵ_{optimo}) is the optimal damping of the TMD, (ω_a) describes the angular frequency of the TMD, (KTMD) is the spring stiffness of the TMD system, while (CTMD) is the damping coefficient of the TMD damper.

3.6. Seismische Parameter

Seismic parameters are factors that most influence the earthquakes that must be considered for structural design in order to calculate the forces acting upon the building in accordance with E.030 for safe, earthquake-resistant design. In Table 2, the first seismic parameter is the seismic zoning of Lima with a zone factor Z = 0.45, because Lima is the most seismically affected region in the country. This factor is important for seismic design, because the city is one of the most seismic risk zones in the country. Following E.030 [26], Lima is in zone 4 (red zone), as seen in Figure 8, meaning there is a great likelihood of seismic activity occurring in the area. The type of occupancy is 1, which is classified as the building having a home, office, or a hotel, which is indicated to have no consequential ancillary fires or the release of noxious materials. The zone is given a 2.5 as the expected seismic amplification factor due to the likelihood of the seismic activity in the area experiencing an increase. The soil classification is rigid (S1 = 1), which is a factor in the expected seismic movements of the building. The Tp(s) C factor is 0.4, the Tl, the C factor zone shift period with constant displacement, is 2.5. The expected seismic activity of the building has an inward corner irregularity of 0.90 correction factor. For the building with a system attribute of dual reining, the seismic reduction coefficient (R0) is established to 7, allowing the building to withstand considerable tremors [26].

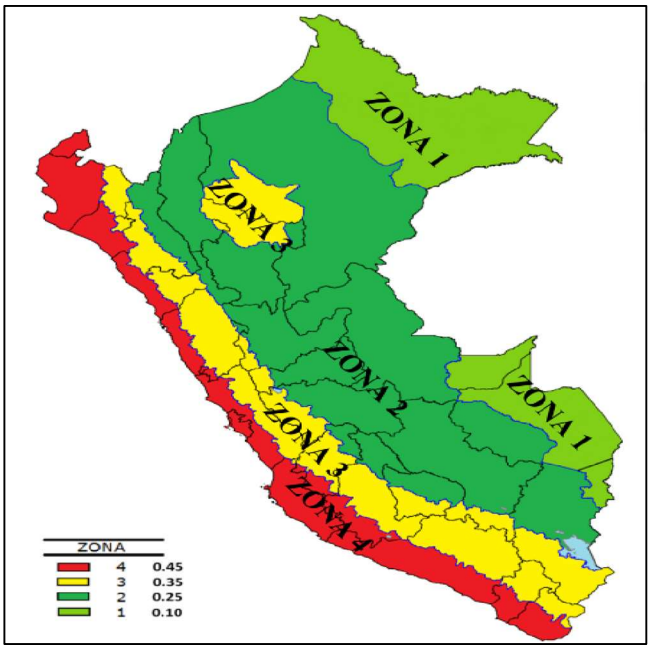

Fig. 8 Seismic zones in Peru [26]

Table 2. Seismic parameters [26]

Seismic parameters	Factor
Z (zone factor)	0.45
U (use factor)	1
C (seismic amplification factor)	2.5
S1 (Soil factor)	1
Tp (period defining the C-factor platform)	0.4
Tl (period defining the start of the C factor zone with constant displacement)	2.5
Irregularity due to inward corners	0.90
R (Seismic reduction coefficient factor)	7

Using the data provided in Table 1, the spectral acceleration was calculated using equation 9 [26], which is essential for determining the dynamic demand that will act on the structure. This spectral acceleration allows the estimation of the lateral forces that the structure must be able to withstand. Based on this estimate, the structure's capacity to withstand these forces can be evaluated, which is essential to ensure that the design complies with the requirements established by Peruvian Technical Standard E.030. This analysis is therefore a crucial step in the structural design process, ensuring that the building is adequate to withstand lateral loads safely and efficiently.

$$S_a = \frac{Z.U.C.S}{R}.g \tag{9}$$

Where (Z) represents the zone factor that characterises the seismic severity of the study area, (U) corresponds to the use factor associated with the importance and function of the building, (C) denotes the seismic amplification factor that depends on the type of structure and its dynamic response, (S) is the soil factor that reflects the geotechnical conditions, (R) indicates the seismic force reduction coefficient, and (g) represents the acceleration due to gravity.

Figure 9 shows the structures designed in ETABS, which were modelled using the seismic parameters specified in Table 2. Item A corresponds to a 10-story structure, item B to a 15-story structure, and item C to a 20-story structure. Subsequently, TMD (Tuned Mass Damper) and DFV (Chevron Brace Viscous Force Device) were applied to these models.

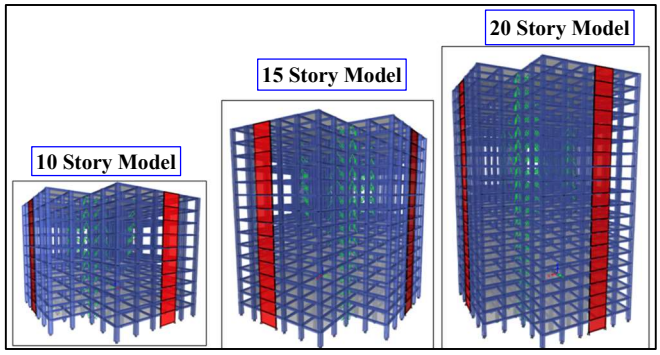

Fig. 9 Structural models modelled in ETABS (10, 15, and 20 storeys)

Table 3 shows the properties of the viscous fluid device in Chevron Brace configuration for the different 10-story structures, including the floor height, the stiffness of the metal arm (k), the velocity exponent (α), and the non-linear damping coefficient (c_{iy}) corresponding to each number of storeys, the values of which are detailed below.

Table 3. Properties of viscous fluid in the chevron brace arrangement

Number of floors	Story height (m)	Metal arm stiffness (k)	Velocity exponent (α)	Non-linear damping coefficient (ciy)
10	3.00	96051.94	0.50	323.14
11	3.00	96051.94	0.50	98.86
12	3.00	96051.94	0.50	228.46
13	3.00	96051.94	0.50	266.51
14	3.00	96051.94	0.50	309.63
15	3.00	96051.94	0.50	304.65
16	3.00	96051.94	0.50	307.13
17	3.00	96051.94	0.50	363.77
18	3.00	96051.94	0.50	442.47
19	3.00	96051.94	0.50	436.17
20	3.00	96051.94	0.50	263.79

Table 4 shows the properties of the tuned mass used in this study, where it was determined that the optimum percentage of tuned mass is 10% of the total mass of the structure. This value was used as the basis for the analysis of structures with 10 to 20 floors. It can be seen that, as the number of storeys increases, the tuned mass (ma) increases progressively, which implies an adaptation of the control system to the increasing total mass of the structure. Likewise, the stiffness (Ka) and damping (Ca) values tend to decrease with the number of storeys, reflecting the adjustment necessary to maintain the efficiency of the tuned mass system in the face of variations in the dynamic properties of the structure.

Table 4. Properties of tuned mass

Number of floors	No. of floors Optimum Percentage of Tuned Mass 10%		
	Stiffness (Ka)	Damping (Ca)	Mass (ma)
10	2042.08	174.82	104.27
11	1617.88	154.80	103.19
12	1657.94	163.48	112.31
13	1654.07	179.65	135.93
14	1492.97	177.19	146.50
15	1357.20	174.93	157.08
16	1243.74	173.00	167.65
17	1145.47	171.18	178.22
18	1060.50	169.52	188.79
19	987.10	168.07	199.36
20	922.40	166.72	209.93

4. Results

4.1. Chevron Brace Arrangement

4.1.1. Maximum Displacements in Structures from 20 to 16 Storeys

Table 5 shows that the maximum displacements decreased in all cases when the viscous fluid dissipator was incorporated into the Chevron Brace configuration. In the building with 16 storeys, the displacement was reduced from 0.285196 m to 0.222158 m because the internal fluid generated resistance proportional to the piston velocity, transforming part of the kinetic energy into heat and reducing the vibration amplitude. In the building with 17 storeys, the displacement decreased from 0.365807 m to 0.228229 m, as the longer structural period allowed the damper to operate more effectively, increasing viscous dissipation. In the building with 18 storeys, the variation from 0.430060 m to 0.225467 m was due to the optimal use of the piston stroke and the alignment of the Chevron system with the main load trajectories, which stabilised the lateral movement. In the building with 19 storeys, the change from 0.455830 m to 0.233075 m showed the highest level of control, resulting from the increased relative velocity and accumulated energy at the upper levels, which enhanced the power dissipated per cycle. Finally, in the building with 20 storeys, the displacement decreased from 0.453164 m to 0.248635 m, maintaining a high degree of control thanks to the large modal

mass and the non-linear behaviour of the fluid, although slight torsional effects limited its efficiency compared with the building with 19 storeys.

Table 5. Maximum displacements

Storey	Without dissipator (m)	With dissipator (m)	% Reduction
16	0.285196	0.222158	22.103%
17	0.365807	0.228229	37.609%
18	0.43006	0.225467	47.573%
19	0.45583	0.233075	48.868%
20	0.453164	0.248635	45.134%

Figure 10 illustrates how displacement curves showed a distinct downward trend with more storeys, indicating the increased efficiency of the system in the dissipation of energy. The percentage decreases were 22.103% in buildings with 16 storeys, 37.609% in buildings with 17 storeys, 47.573% in buildings with 18 storeys, 48.868% in buildings with 19 storeys, and 45.134% in buildings with 20 storeys, showing an upward trend up to 19-storeys followed by a slight reduction in the building with 20-storeys. This variation indicated that the viscous-fluid system in the Chevron Brace configuration achieved its maximum effectiveness in the buildings with 18 and 19 storeys, where the combination of greater modal mass and a longer structural period allowed for more intense and continuous energy dissipation. The visual comparison between the curves of the structures with the device (CD) and without the device (ND) confirmed that the widest separations occurred in the buildings with 18 and 19 storeys, whereas the buildings with 16, 17, and 20 storeys showed narrower separations, reflecting a less pronounced reduction. Overall, the figure showed that the control capacity of the system increased proportionally with the dynamic demand and with the relative displacement between levels, reaching optimal performance in the taller buildings analysed.

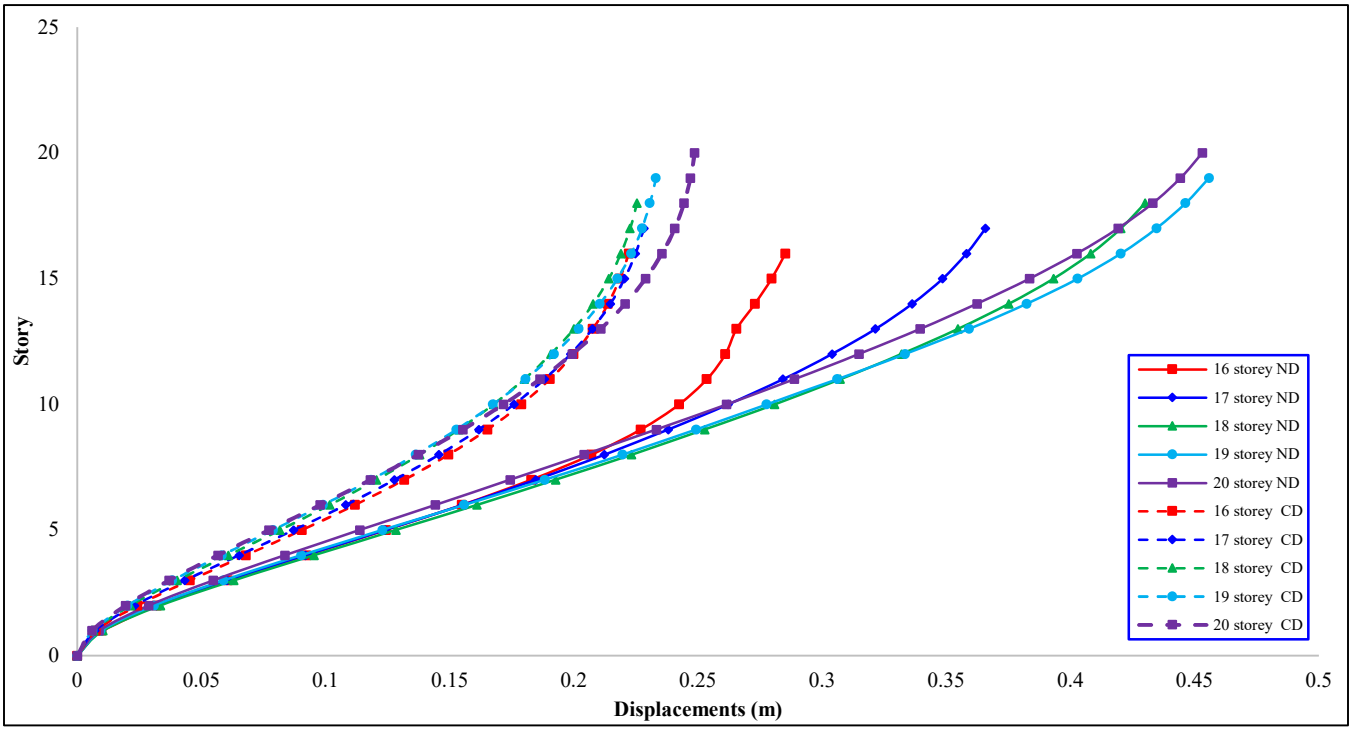

Fig. 10 Maximum displacements in structures from 20 to 16 storeys

4.1.2. Maximum Displacements in Structures with 15 to 10 Storeys

Table 6 shows that maximum displacements decreased steadily when the viscous fluid damper was incorporated into the Chevron Brace arrangement. On 10 floors, displacement was reduced from 0.211707 m to 0.084829 m because the damper acted with high efficiency, exhibiting low stiffness response and higher relative velocities between nodes, allowing for optimal energy dissipation. On 11 floors, the displacement decreased from 0.210694 m to 0.173965 m, showing a smaller reduction due to the stiffer behaviour of the system and the lower relative deformation available for fluid activation. On 12 floors, the change from 0.260793 m to 0.172789 m showed a significant improvement as the amplitude of lateral movement and modal participation increased. On 13 floors, displacement decreased from 0.283580 m to 0.186279 m, reflecting adequate utilisation of the viscous damping mechanism thanks to the increased piston travel and axial alignment of the Chevron system. At 14 storeys, the value decreased from 0.269875 m to 0.187164 m,

maintaining stable control through the combination of structural rigidity and dissipation capacity. Finally, at 15 storeys, the displacement went from 0.270570 m to 0.199793 m, showing a sustained reduction that was explained by the balance between the dissipated energy and the dynamic demand of the structure. Taken together, these results demonstrated that the action of the viscous fluid reduced the maximum displacements by absorbing part of the vibrational energy and transforming it into heat through internal shear stresses, with a more noticeable performance in the models with lower rigidity and greater relative displacement.

Table 6. Maximum displacements

Story	Without dissipator	With dissipator	% Reduction
10	0.211707	0.084829	59.931%
11	0.210694	0.173965	17.432%
12	0.260793	0.172789	33.745%
13	0.28358	0.186279	34.312%
14	0.269875	0.187164	30.648%
15	0.27057	0.199793	26.158%

In Figure 11, the reduction percentages showed variable behaviour with values of 59.931% on 10 floors, 17.432% on 11 floors, 33.745% on 12 floors, 34.312% in 13 storeys, 30.648% in 14 storeys, and 26.158% in 15 storeys, with maximum efficiency observed in the 10-storey structure and a gradual decrease in taller structures. The comparison between the curves of structures with dissipators (CD) and without dissipators (ND) showed wider separations in the 10-storey model, where greater flexibility allowed for greater damper work, while the separations progressively decreased between 11 and 15 storeys, confirming that the control of the viscous fluid depended directly on the magnitude of the relative displacement and the kinetic energy generated at each structural level.

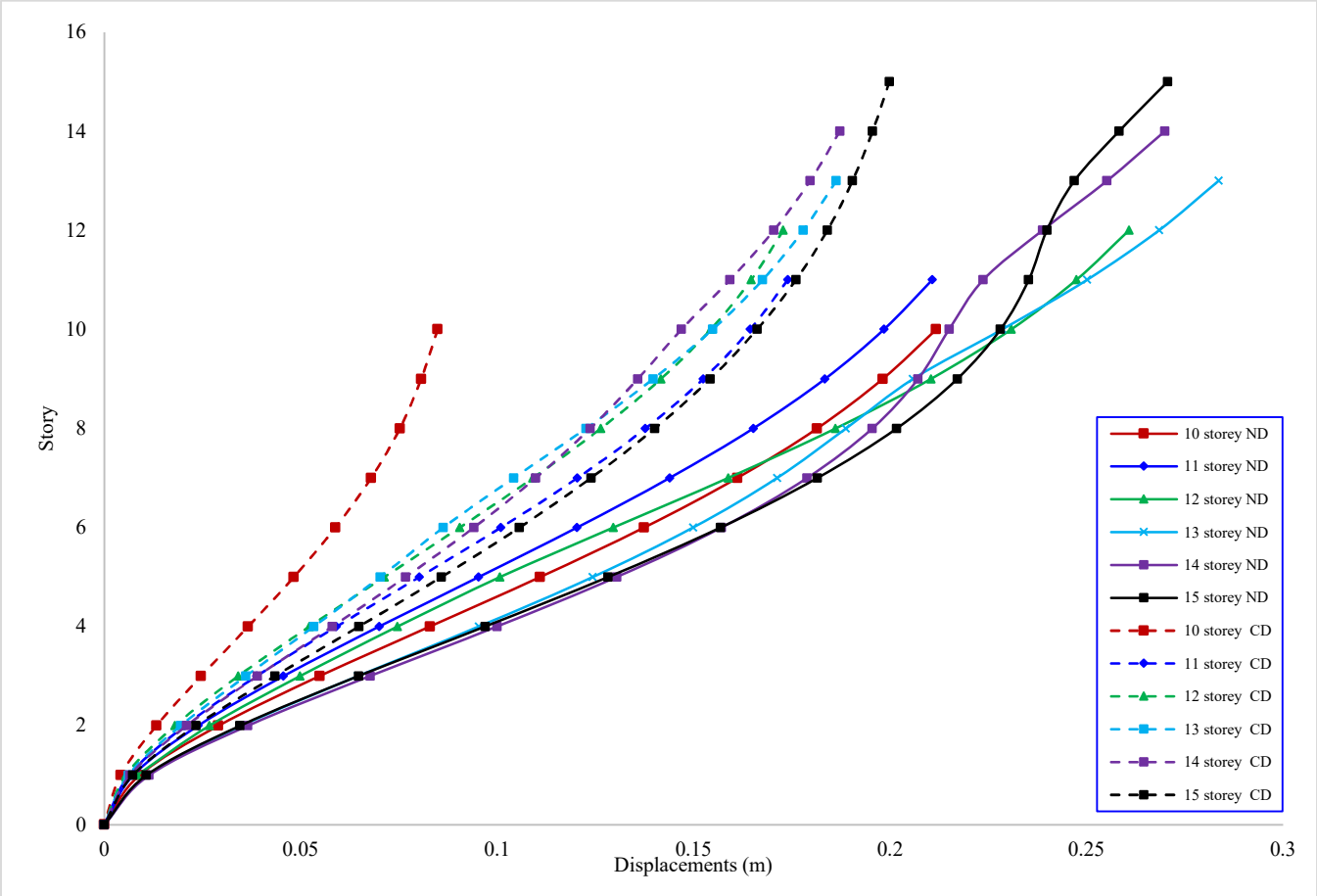

Fig. 11 Maximum displacements in structures with 15 to 10 storeys

4.1.3. Drift in Structures from 20 to 16 Storeys

Table 7 shows that drift decreased significantly with the incorporation of the viscous fluid dissipator in a Chevron Brace arrangement, reflecting an improvement in the dynamic stiffness of the structure. In 16-storey buildings, drift was reduced from 0.01071 to 0.007588, demonstrating efficient control of lateral deformations through the action of the fluid, which absorbed part of the kinetic energy generated by the seismic movement. On 17 floors, the drift decreased from 0.010885 to 0.007387 due to the increase in effective damping

that limited the angular response and torsional rotation of the upper levels. On 18 floors, the value went from 0.011286 to 0.006979, showing that the device dissipated more energy as the relative displacement between floors increased, stabilising the structure without generating excessive stress. At 19 storeys, the drift was reduced from 0.011162 to 0.006895, maintaining controlled and uniform behaviour throughout the height thanks to the combined work of the Chevron system and the viscous fluid. Finally, in the case of 20 storeys in height, the drift went from the value of 0.010314 to the value of 0.006993, ascertaining the removal of the structural deficiency of the hovering of the storeys by lessening the hovering of the storeys and eliminating the locking of the deformations at the middle levels. As a whole, results showed that the added dissipator, the damping of the structural system was augmented, controlling drift to a lower value, and certifying a more uniform and less unpredictable seismic performance.

Table 7. Drifts in structures from 20 to 16 storeys

Story	Without dissipator	With dissipator	% Reduction
16	0.01071	0.007588	29.15%
17	0.010885	0.007387	32.14%
18	0.011286	0.006979	38.16%
19	0.011162	0.006895	38.23%
20	0.010314	0.006993	32.20%

In Figure 12, the values for the decrease percentages showed a decent amount of change in a steady manner, with the values being 29.15% at 16 storeys, 32.14% at 17 storeys, 38.16% at 18 storeys, 38.23% at 19 storeys, and 32.20% at 20 storeys, showing the cumulative increasing effectiveness of the dissipator system with increase in height and structural flexibility, and the values being moderate showed a decent amount of change in a steady manner.

The drift of the values at the structures with the dissipators (CD) was comparatively close to the vertical axis, depicting a lesser amount of frictioned drift compared to the structures that did not have dissipators (ND). The greatest separations between curves were observed in the 18- and 19-storey models, where the viscous fluid achieved its maximum energy performance, taking advantage of the higher relative speeds of the pistons.

In the 16- and 17-storey models, the reduction was smaller, although sufficient to demonstrate effective deformation control. In the 20-storey model, the trend remained stable, showing a balance between stiffness, damping, and relative displacement.

Overall, the figure showed that the use of the dissipator significantly reduced maximum drifts, homogenised the dynamic response, and improved the overall stability of the structure under seismic loads.

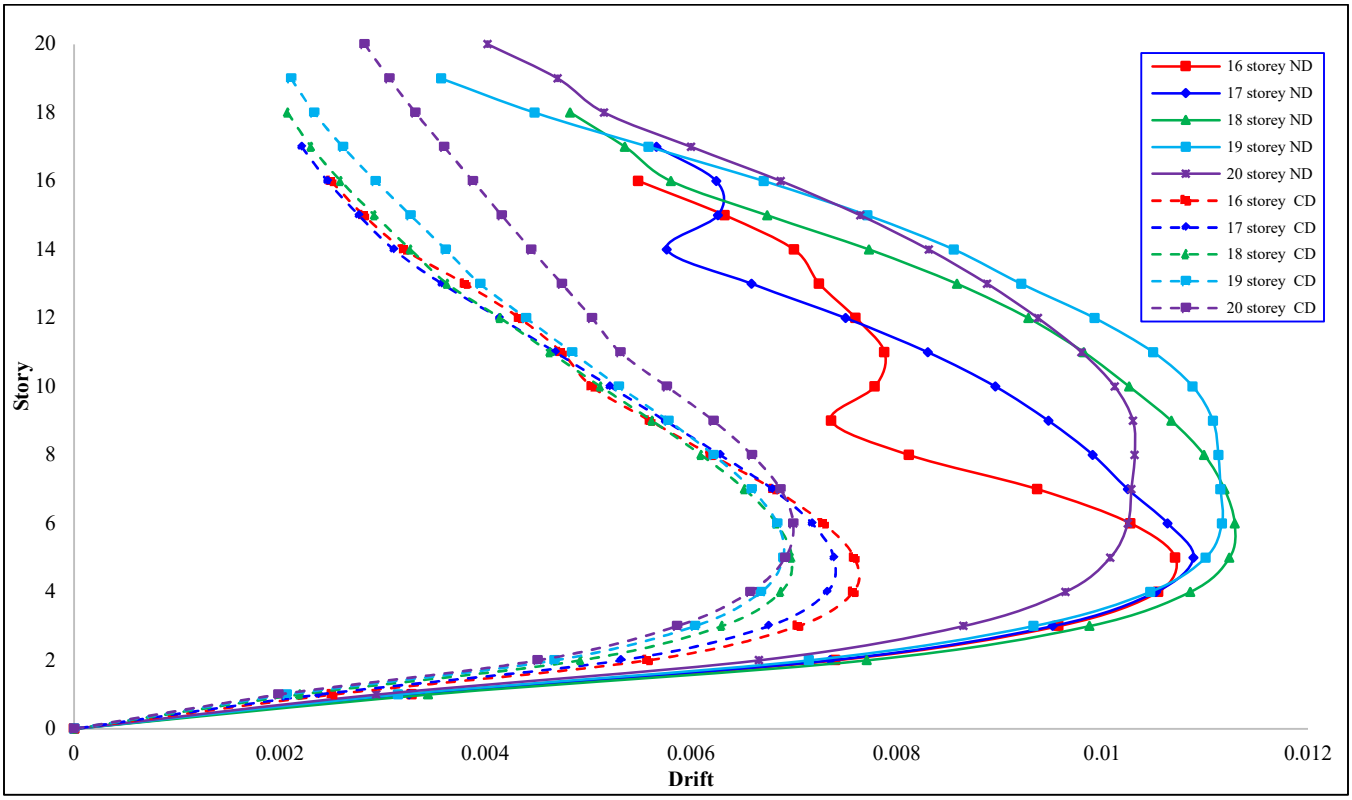

Fig. 12 Drift in structures from 20 to 16 storeys

4.1.4. Drift in 15 to 10 Storey Structures

Table 8 shows that inter-storey drift decreased in all models when the Chevron Brace viscous fluid dissipator was incorporated. In 10-storey buildings, drift decreased from 0.009356 to 0.004068 because the damper operated at higher relative velocities and transformed part of the kinetic energy into heat, restricting lateral response. In 11 storeys, it decreased from 0.008573 to 0.007174 due to the increase in effective damping and the axial trajectory of the brace, which reduced rotation at the nodes. On 12 floors, the drift was reduced from 0.009936 to 0.006562, as the piston travel was better utilised as the modal participation increased. On 13 floors, it decreased from 0.010257 to 0.006377 because viscous dissipation per cycle was greater and cumulative drift stabilised throughout the height. On 14 floors, it decreased from 0.010787 to 0.006355, reflecting higher effective dynamic stiffness due to the combined action of the fluid and the Chevron. On 15 floors, it went from 0.010745 to 0.007136, maintaining deformation control by balancing dynamic demand with dissipation capacity.

Table 8. Drifts in structures from 15 to 10 storeys

Storey	Without dissipator	With dissipator	% Reduction
10	0.009356	0.004068	56.52%
11	0.008573	0.007174	16.32%
12	0.009936	0.006562	33.96%
13	0.010257	0.006377	37.83%
14	0.010787	0.006355	41.09%
15	0.010745	0.007136	33.59%

Figure 13 shows that the reduction percentages demonstrated favourable and progressive behaviour of the viscous fluid dissipator system in the Chevron Brace configuration, with values of 56.52% on 10 floors, 16.32% on 11 floors, 33.96% on 12 floors, 37.83% on 13 floors, 41.09% on 14 floors, and 33.59% on 15 floors. In the graph, the curves corresponding to the structures with dissipators (CD) were closer to the vertical axis than those without dissipators (ND), reflecting a notable decrease in lateral drift and better control of the structural response. The greatest separations between curves occurred in the 10-, 13-, and 14-storey models, coinciding with the peaks of system efficiency, where the energy dissipated by the fluid effectively limited the relative deformations between levels. In contrast, in the 11- and 15-storey models, the difference was smaller, although sufficient to maintain structural control within the optimal damping range. Overall, the figure showed that the incorporation of the dissipator favoured a uniform redistribution of drift, reduced critical concentrations of deformation, and maintained a stable and predominantly elastic structural response to seismic excitations, reinforcing its effectiveness as a passive seismic control system in medium-rise buildings.

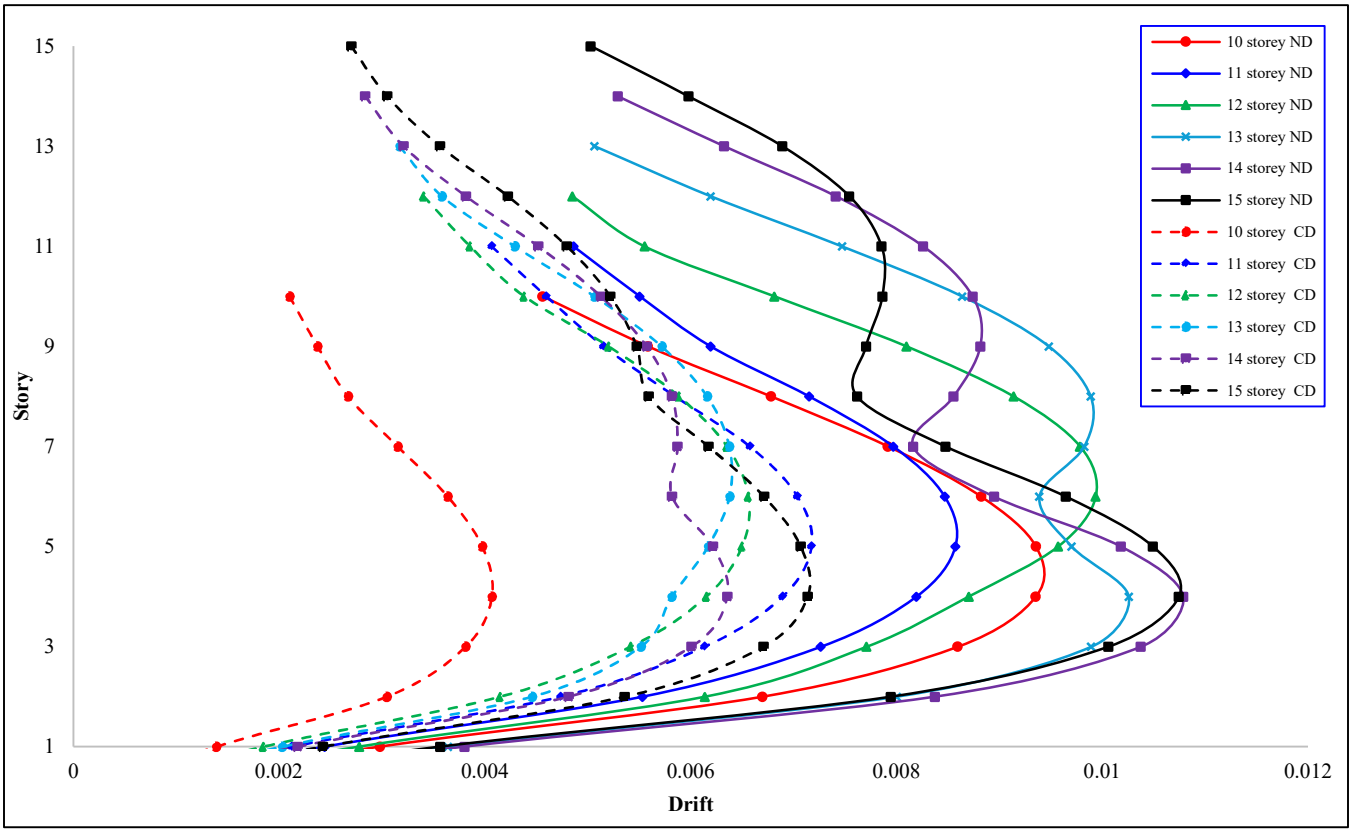

Fig. 13 Drift in structures from 15 to 10 storeys

4.1.5. Accelerations in Structures from 20 to 16 Storeys

Table 9 shows that the maximum acceleration decreased consistently in all structures when the viscous fluid dissipator was incorporated into the Chevron Brace configuration. On 16 floors, the value went from 7.3679 m/s² to 5.4114 m/s² due to the viscous resistance generated by the piston displacement, which absorbed part of the energy transmitted from the base to the upper levels.

On 17 floors, acceleration was reduced from 7.1229 m/s² to 5.3431 m/s², demonstrating the system's effective control of horizontal oscillations by dissipating kinetic energy into heat. On the 18th floor, the value dropped from 7.7796 m/s² to 5.3125 m/s², which was attributed to optimal use of the fluid's compression and expansion cycle, which limited vibrations on the intermediate floors.

On 19 floors, the acceleration dropped from 7.9628 m/s² to 5.2996 m/s², demonstrating the greater stability of the model, as the fluid reached a constant dissipation regime in the face of peak accelerations induced by the seismic load. Finally, on 20 floors, acceleration decreased from 7.5618 m/s² to 5.4117 m/s², confirming that the dissipator contributed to reducing energy transfer between levels and smoothing the dynamic response of the structure.

Taken together, these results demonstrated that the Chevron Brace system with viscous fluid acted as a passive control element that limited local accelerations, improved structural comfort, and reduced internal stresses caused by seismic excitation.

Table 9. Aceleraciones en estructuras de 20 a 16 pisos

Story	Without dissipator (m/s²)	With dissipator (m/s²)	% Reduction
16	7.3679	5.4114	26.554%
17	7.1229	5.3431	24.987%
18	7.7796	5.3125	31.712%
19	7.9628	5.2996	33.446%
20	7.5618	5.4117	28.434%

Figure 14 shows that the percentages of maximum acceleration reduction exhibited uniform and progressive behaviour, with values of 26.554% on 16 floors, 24.987% on 17 floors, 31.712% on 18 floors, 33.446% on 19 floors, and 28.434% on 20 floors, reflecting a general trend of improvement in structural stability. The curves corresponding to the models with dissipators (CD) were consistently below those without dissipators (ND), especially on the upper floors, where the difference between the two was greater.

This behaviour indicated that the device effectively reduced the accelerations transmitted to the structure by acting as a viscous damper that attenuates high-frequency vibrations. It was also observed that the 18- and 19-storey models had the greatest separation between curves, which coincided with the highest reduction percentages and demonstrated a more controlled response to seismic loads. In contrast, the 16, 17, and 20-storey structures showed a more moderate reduction, although they maintained the downward trend in accelerations with the incorporation of the system.

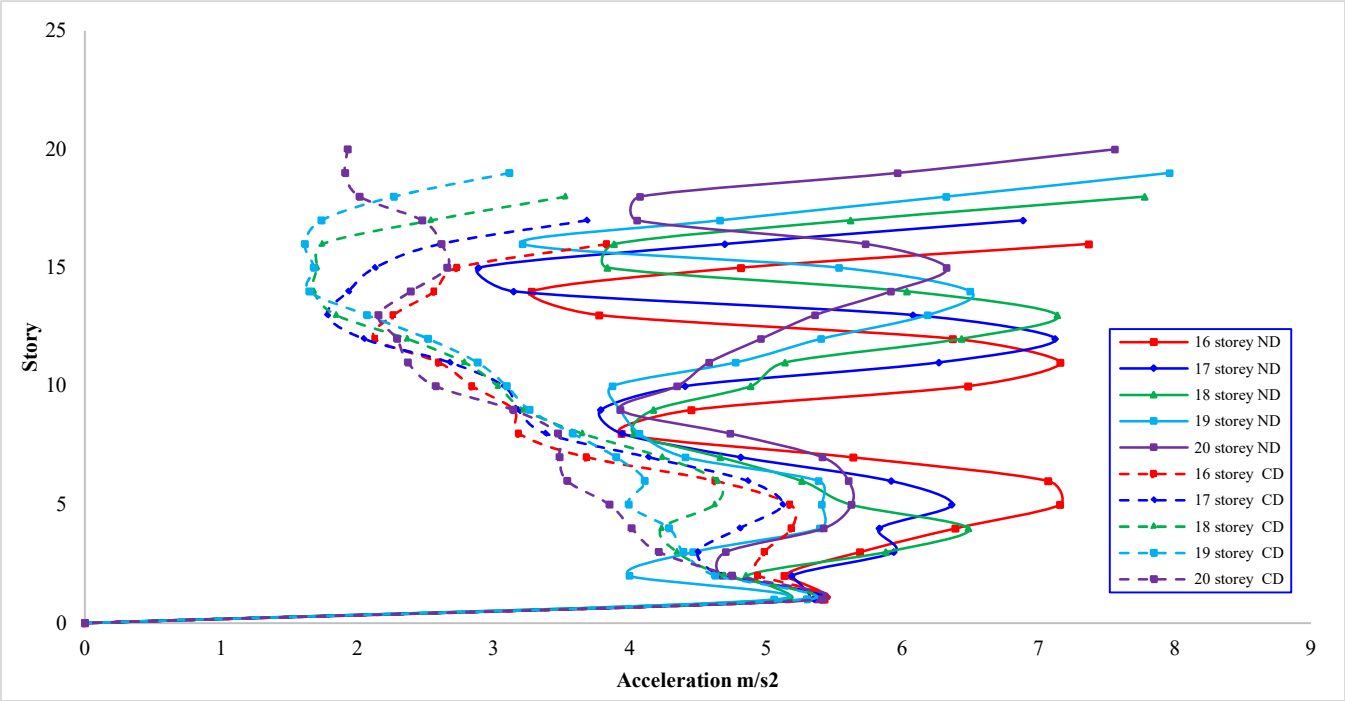

Fig. 14 Accelerations in structures from 20 to 16 storeys

4.1.6. Accelerations in Structures from 15 to 10 Storeys

Table 10 shows that maximum acceleration decreased significantly in all models when the viscous fluid dissipator was implemented in a Chevron Brace configuration. On 10 floors, acceleration went from 16.9991 m/s² to 7.0671 m/s², showing a substantial reduction due to the high relative speed between nodes, which allowed for effective energy dissipation through the fluid. On 11 floors, the value decreased from 13.2935 m/s² to 9.1746 m/s², demonstrating that the viscosity of the fluid acted as a dynamic damper that softened local accelerations. On the 12th floor, the decrease from 11.3366 m/s² to 5.9131 m/s² reflected optimal system performance, maintaining an adequate balance between the rigidity of the diagonals and the viscous resistance of the piston. On 13 floors, the acceleration dropped from 10.0937 m/s² to 5.4395 m/s², confirming the device's ability to reduce inertial forces on intermediate floors by converting kinetic energy into heat. On 14 floors, the value decreased from 8.3667 m/s² to 5.4232 m/s², maintaining a controlled response to seismic excitation. Finally, on 15 floors, the acceleration went from 9.299 m/s² to 5.4902 m/s², showing stable behaviour and less vibration propagation to the upper part.

Table. 10 Aceleraciones en estructuras de 15 a 10 pisos

Story	Without dissipator (m/s²)	With dissipator (m/s²)	% Reduction
10	16.9991	7.0671	58.427%
11	13.2935	9.1746	30.984%
12	11.3366	5.9131	47.841%
13	10.0937	5.4395	46.110%
14	8.3667	5.4232	35.181%
15	9.299	5.4902	40.959%

Figure 15 shows that the reduction percentages reached 58.427% in buildings with 10 storeys, 30.984% in buildings with 11 storeys, 47.841% in buildings with 12 storeys, 46.110% in buildings with 13 storeys, 35.181% in buildings with 14 storeys, and 40.959% in buildings with 15 storeys, revealing a general trend of effective system control, with a greater impact on the lower buildings. The curves corresponding to the structures with dissipators (CD) shifted towards lower acceleration values compared with those without dissipators (ND), reflecting a clear reduction in the dynamic response. In the buildings with 10 and 12 storeys, the differences between curves were the greatest, indicating that in these configurations the system achieved its highest dissipation efficiency. In the buildings with 13 and 15 storeys, the curves remained significantly separated, confirming that the viscous-fluid system remained stable despite the increase in modal mass and structural stiffness. Conversely, in the buildings with 11 and 14 storeys, the reductions were more moderate, associated with the lower displacement amplitudes and, consequently, the lower relative velocity in the pistons. Overall, the figure showed that the viscous-fluid system in the Chevron Brace arrangement not only reduced peak accelerations at all levels but also homogenised the structural response, preventing critical dynamic concentrations and enhancing dissipation capacity in mid-rise buildings.

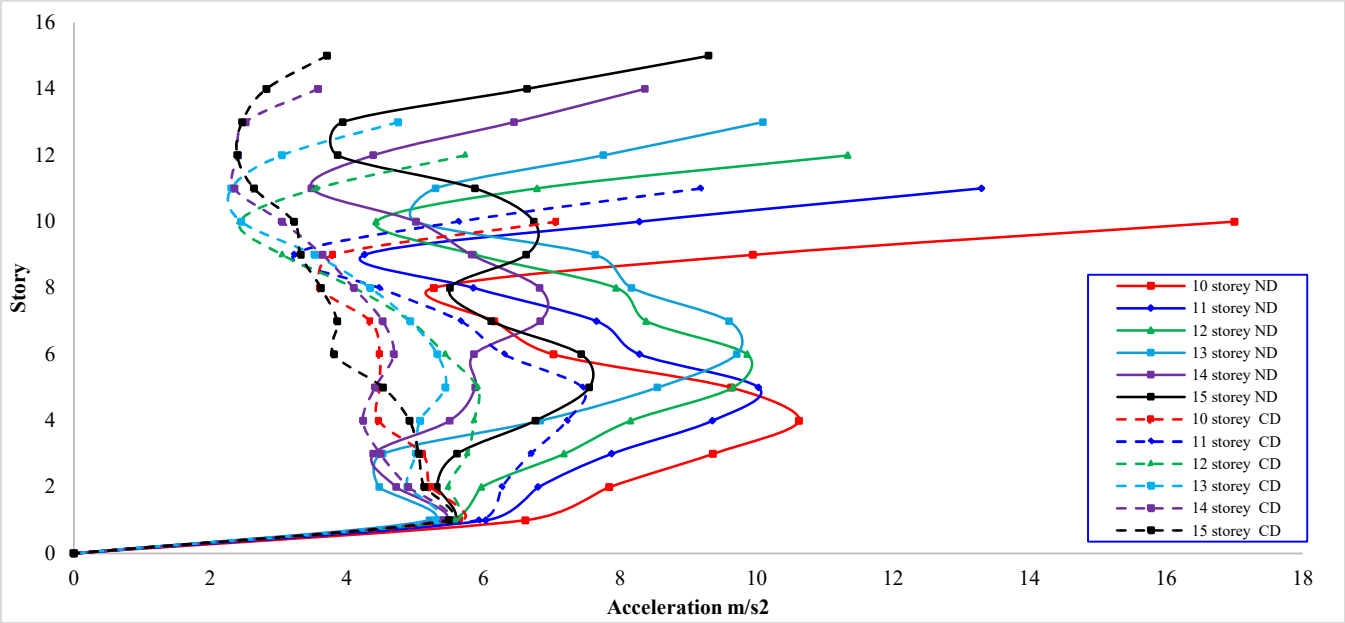

Fig. 15 Accelerations in structures from 15 to 10 storeys

4.1.7. Shear Force at the Base

Table 11 shows that the shear force at the base decreased considerably in all buildings when the viscous fluid dissipator was incorporated in the Chevron Brace configuration, confirming its efficiency in reducing seismic demands. On 10 floors, the force decreased from 2118.18 tonnes to 1465.5889 tonnes as a result of viscous dissipation, which reduced the transfer of forces from the base to the upper levels. On the 11th floor, it decreased from 2,250.77 tonnes to 1,651.6936 tonnes, while on the 12th floor, it decreased from 2,096.63 tonnes to 1,533.0273 tonnes, showing that the system managed to absorb a significant part of the input energy. On 13 floors, the decrease from 2,844.27 tonnes to 1,475.0434 tonnes represented one of the largest absolute differences, resulting from the increase in the work of the damper when reaching greater relative displacements. Over the course of 14 floors, the mass mitigation was brought down from 3188.76 tonnes to 1666.6615 tonnes. This greatly indicates improved control thanks to the increased dynamic stiffness of the bracing. Over the course of 15 floors, the mass mitigation was dropped from 3356.45 tonnes to 1919.984 tonnes, indicating that the fluid was working within its optimal damping range. Over the course of 16 floors, the mass mitigation decreased from 3056.67 tonnes to 1908.6544 tonnes, illustrating that there existed an optimal balance between the capacity for dissipation and the seismic demand. At 17 storeys, the shear force decreased from 2892.81 tonnes to 1676.81 tonnes, demonstrating the stabilisation of lateral behaviour. At 18 storeys, the variation from 2991.77 tonnes to 1590.53 tonnes showed the effectiveness of the system in reducing reaction peaks at the base. On the 19th floor, the weight of the structure decreased from 3037.74 tonnes to 1698.8684 tonnes, and on the 20th floor, from 2799.73 tonnes to 1892.3279 tonnes, thus confirming a more reasonable and controlled weight. Overall, the calculated values of viscous fluid and energy damped the effective structural stiffness perceived at the base, decreased the seismic energy transmission to the main structure, and thus, prevented excessive force concentrations at the structural supports.

Table 11. Fuerza cortante en la base

Storey	Without dissipator	With dissipator	% Reduction
10	2118.18	1465.5889	30.81%
11	2250.77	1651.6936	26.62%
12	2096.63	1533.0273	26.88%
13	2844.27	1475.0434	48.14%
14	3188.76	1666.6615	47.73%
15	3356.45	1919.984	42.80%
16	3056.67	1908.6544	37.56%
17	2892.81	1676.81	42.04%
18	2991.77	1590.53	46.84%
19	3037.74	1698.8684	44.07%
20	2799.73	1892.3279	32.41%

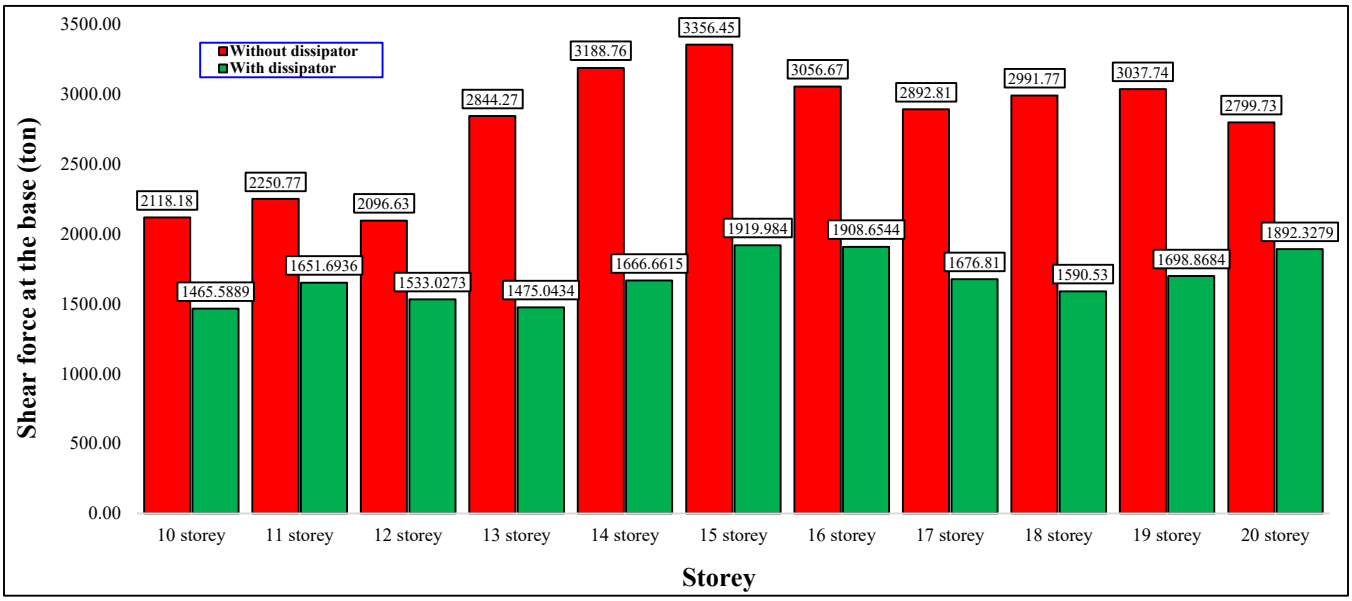

Fig. 16 Shear force at the base

The interval from 26.62% and 48.14% were the range of the reduction percentages found in Figure 16. The biggest values were from buildings 13, 14, 15, 18, and 19 storeys. They managed to achieve values of reductions of 48.14%, 47.73%, 42.80%, 46.84%, and a 44.07% respsectively. In these results, the seismic response was controlled to a greater extent in the mid-rise buildings, and the energy absorbed by the fluid was enough to counter the structural mass of the inertia. 10, 11, and 12-storey buildings had moderate reductions of 30.81%, 26.62%, and 26.88%, and a lower contribution was shown by the dissipator due to the demand for contraction being lower. On the contrary, the 16 and 20-storey buildings had percentages of 32.41% and 44.07%, and on the other hand, there were more slender structures, so there was uniform and controlled behaviour. In the bar chart, there was a consistently lower green column assigned to the structures that had the seismic devices than the larger red columns assigned to the structures that did not have the seismic devices. This showed that the downward trend in the force that was passed to the base was clearly shown, and it was the reason that the damping system not only diminished the seismic forces but also equalized the distribution. Hence, it was shown that the system was arranged in a way that the abrupt shear peaks would be contained, and stability was improved.

4.2. TMD Devices

4.2.1. Maximum Displacements in Structures with 20 to 16 Storeys

Table 12 shows that the use of the tuned mass device (TMD) significantly reduced the maximum displacements in all the structures analysed, demonstrating efficient dynamic control in tall buildings. On 16 floors, displacement decreased from 0.2852 m to 0.1541 m, as a result of the counterphase effect generated between the main mass of the structure and the tuned mass, which absorbed part of the vibration energy. On the 17th floor, the value was reduced from 0.3658 m to 0.1608 m, because the natural frequency of the TMD coincided with the predominant frequency of the building, maximising the transfer of energy to the damper. On the 18th floor, the displacement decreased from 0.4301 m to 0.1724 m, demonstrating optimal system performance, as the tuned mass operated within its resonance range and reduced the amplitude of oscillation. On the 19th floor, the decrease from 0.4558 m to 0.1811 m showed that the TMD continued to maintain effective coupling, generating movement in the opposite direction to that of the structure and thus reducing lateral deformations. Displacement over the 20 floors ranged from 0.4532 m to 0.1832 m, validating the device's capacity to mitigate the building settling during vibrations and confirming the device's utility in high-rise building construction. The results showed the TMD to be a passive control system that reduces the amplitude of structural response by adjusting structural parameters, mass, stiffness, and damping, and shifting the system to a lower amplitude during resonance pumping by the seismic wave in the system. TMD was then effective.

Table 12. Maximum displacements

Story	Without TMD (m)	With TMD (m)	% Reduction
16	0.2852	0.1541	45.98%
17	0.3658	0.1608	56.05%
18	0.4301	0.1724	59.90%
19	0.4558	0.1811	60.27%
20	0.4532	0.1832	59.58%

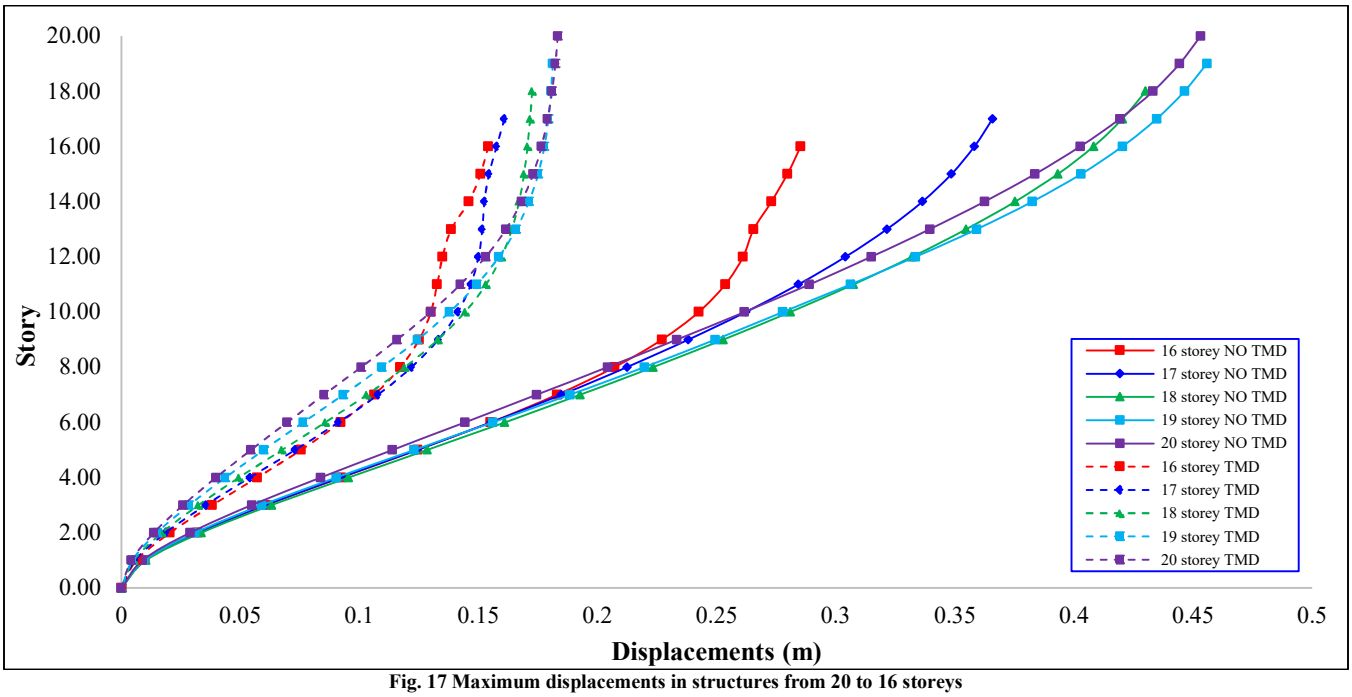

Fig. 17 Maximum displacements in structures from 20 to 16 storeys

In Figure 17, the reduction percentages showed increased values by height of the structure: 45.98% for 16, 56.05% for 17, 59.90% for 18, 60.27% for 19, and 59.58% for 20 floors in the building. Thus, the efficiency of TMD is height and structural flexibility. The curves with and without TMD were observed to be shifted laterally, confirming lower unrestrained lateral displacement due to TMD. For 18 and 19-storey buildings, the lateral shifts were maximal and were observed to be the peaks of the system. 16 and 17-storey buildings were also observed, having a system controlling the response effectively, though the initial response was less than that of buildings with greater storeys. In the case of 20 storeys, the trend remained stable, demonstrating that the TMD retained its damping capacity even in buildings with greater mass and a longer fundamental period. Overall, the figure showed that the incorporation of the TMD promoted a uniform redistribution of deformations along the height, reduced relative accelerations, and kept the structure within the elastic range of behaviour.

4.2.2. Maximum Displacements in Structures with 15 to 10 Storeys

Table 13 shows that the installation of the tuned mass damper (TMD) significantly reduced the maximum displacements in all the buildings evaluated. On 10 floors, displacement was reduced from 0.2117 m to 0.0930 m as a result of the action of the tuned mass, which oscillated in antiphase with the main structure, partially cancelling out the vibration energy. On 11 floors, the value went from 0.2107 m to 0.1041 m, reflecting the TMD's ability to capture energy in the first vibration mode and transform it into controlled displacement. On the 12th floor, the decrease from 0.2608 m to 0.1210 m showed that the tuning frequency of the system coincided with the dominant frequency of the building, allowing for a controlled resonant response and reducing the maximum amplitude of movement. On the 13th floor, the displacement decreased from 0.2836 m to 0.1276 m, showing an improvement in lateral stability and a decrease in the coupling between translation and torsion. If we take 14 floors, the range of the values decreased from 0.2699 m to 0.1417 m, showing that the values are more evenly controlled throughout the height. In the case of 15 floors, the range of values from 0.2706 m to 0.1449 m confirmed the system's effectiveness at countering the structural resonance while keeping the building in the elastic response window.

Table 1. Maximum displacements

Storey	Without TMD (m)	With TMD (m)	% Reduction
10	0.2117	0.0930	56.07%
11	0.2107	0.1041	50.59%
12	0.2608	0.1210	53.59%
13	0.2836	0.1276	54.99%
14	0.2699	0.1417	47.50%
15	0.2706	0.1449	46.43%

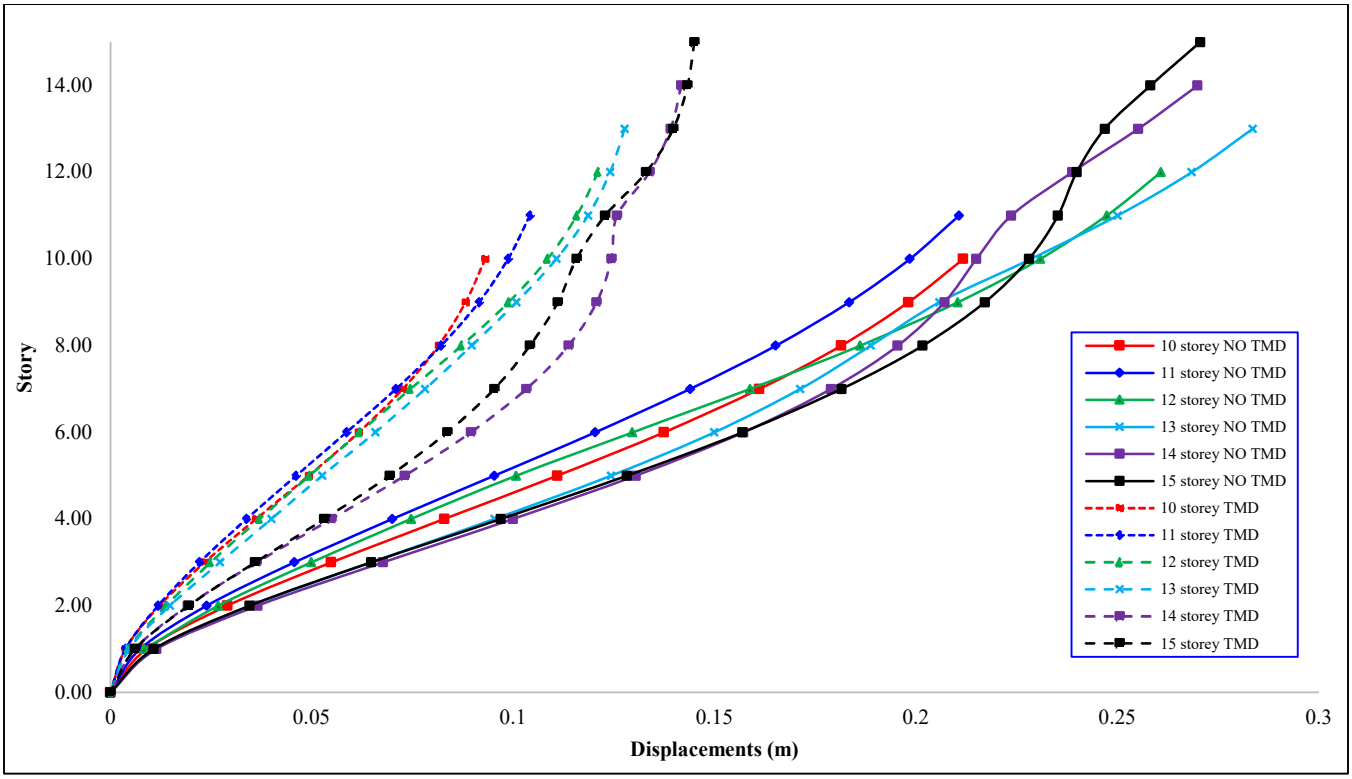

Fig. 18 Maximum displacement in structures with 15 to 10 storeys

As depicted in Figure 18, the reduction percentages exhibited an oscillating tendency, with particularly high reductions in the lower storey buildings column 6.7.1.1. This was followed by an average of 56.07% in ten-storey buildings, 50.59% in eleven-storey buildings, 53.59% in twelve-storey buildings, 54.99% in thirteen-storey buildings, 47.50% in fourteen-storey buildings, and 46.43% in fifteen- storey buildings. Whereas the discontinuous curves of the TMD-configurations were, with no exception, lower than the continuous curves representing the no TMD case, suggesting all around lesser lateral displacements. It was made evident that the ten, eleven, and thirteen-storey buildings were the ones that most concentrated peaks of system efficiency, and tandem with this were the ones that adequately tuned TMD frequency and building natural frequency, so that seismic oscillations were significantly attenuated. On the contrary, fourteen and fifteen-storey buildings exhibited a more subdued response, albeit the system was effective enough in controlling the response so as not to allow high rates of increase in maximum displacement. By and large, the TMD considerably decreased displacement demand, improved the dynamic stability of the system, and dissipated energy through controlled resonance, proving to be a very effective passive device in mid-rise buildings.

4.2.3. Drift in Structures with 20 to 16 Storeys

Table 14 shows that inter-storey drift decreased considerably in all structures when the tuned mass damper (TMD) was incorporated, demonstrating a significant improvement in lateral control and dynamic stiffness of the structural system. In 16-storey buildings, drift was reduced from 0.0107 to 0.0063 as a result of the interaction between the tuned mass and the structure, which generated an inertial force opposite to the movement of the building and reduced relative deformations. On the 17th floor, the value went from 0.0109 to 0.0063, showing similar behaviour, where the TMD acted in resonance with the first vibrational mode, absorbing part of the kinetic energy. On the 18th floor, the reduction from 0.0113 to 0.0061 reflected an increase in the effectiveness of the system, due to the fact that the fundamental period of the building approached the optimal tuning of the device. On 19 floors, the drift decreased from 0.0112 to 0.0057, demonstrating more stable dynamic control thanks to the greater amplitude of movement of the tuned mass and its ability to counteract the torsional response. Finally, on 20 floors, the decrease from 0.0103 to 0.0054 confirmed that the TMD maintained its performance even in more flexible structures, reducing the demand for relative displacement between levels.

Table 2. Drift in structures from 20 to 16 storeys

Storey	Without TMD	With TMD	% Reduction
16	0.0107	0.0063	41.07%
17	0.0109	0.0063	41.86%
18	0.0113	0.0061	45.93%
19	0.0112	0.0057	49.21%
20	0.0103	0.0054	47.54%

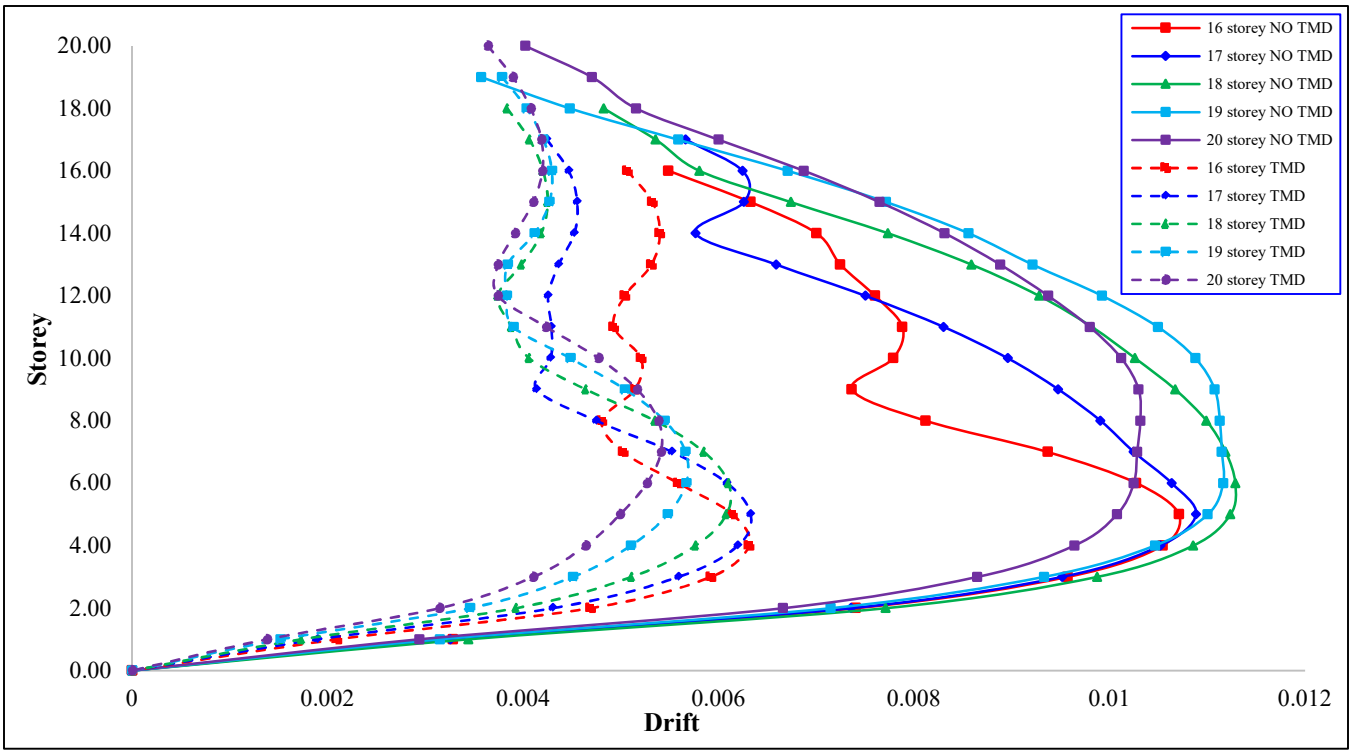

Fig. 19 Drift in structures from 20 to 16 storeys

In Figure 19, the amount of reduction was 41.07% for the 16-storey design, 41.86% for the design containing 17-storeys, 45.93% for the 18-storey case, 49.21% for the 19-storey design, and 47.54% for the design containing 20-storeys, which illustrated an increase that demonstrated the refinement of the energy dissipation tool. Although the building heights increased, the reduction was still proportional and explained the energy dissipation tool's effectiveness for different building heights. The discontinuous curves, corresponding to the configurations with viscous-fluid dampers, consistently remained below the continuous curves (without dampers), indicating a clear decrease in lateral drifts across all levels. The cases with 18 and 19 storeys exhibited the largest separations between curves, matching the highest percentage reduction values and demonstrating that the device operated within its optimal energy-dissipation range. In contrast, the cases with 16 and 17 storeys showed smaller differences, although still sufficient to confirm an increase in effective stiffness and a noticeable reduction in inelastic deformations. Overall, the figure showed that the incorporation of the damper reduced maximum drifts, homogenised the dynamic response between storeys, and improved the global stability of the structure under high-intensity seismic excitations.

4.2.4. Drift in Buildings with 15 to 10 Storeys

Table 15 shows that, in buildings with 10 storeys, the drift decreased from 0.0094 to 0.0044 due to the action of the tuned mass, which oscillated in antiphase with the main structure, reducing the amplitude of relative displacements. In buildings with 11 storeys, the value decreased from 0.0086 to 0.0044, showing that the TMD operated within its optimal resonance range, absorbing part of the kinetic energy induced by the seismic motion. In buildings with 12 storeys, the drift decreased from 0.0099 to 0.0049, indicating a more balanced response due to the tuning between the vibration period of the device and the fundamental mode of the building. In buildings with 13 storeys, the value decreased from 0.0103 to 0.0048, reflecting an improvement in effective dynamic stiffness and a reduction in torsional eccentricity. In buildings with 14 storeys, the drift was reduced from 0.0108 to 0.0062 as a result of the interaction between the tuned mass and the structure, which allowed a more uniform distribution of deformations. Finally, in buildings with 15 storeys, the drift decreased from 0.0107 to 0.0058, confirming that the system maintained consistent and controlled performance, managing to dampen lateral vibrations and limit interstorey distortion. Overall, the values demonstrated that the TMD improved dynamic behaviour by reducing drift in all configurations, contributing to the overall stability of the structure and the protection of its non-structural elements.

Table 15. Drifting in structures from 15 to 10 storeys high

Story	Without TMD	With TMD	% Reduction
10	0.0094	0.0044	53.10%
11	0.0086	0.0044	48.22%
12	0.0099	0.0049	50.48%
13	0.0103	0.0048	52.93%
14	0.0108	0.0062	42.63%
15	0.0107	0.0058	46.37%

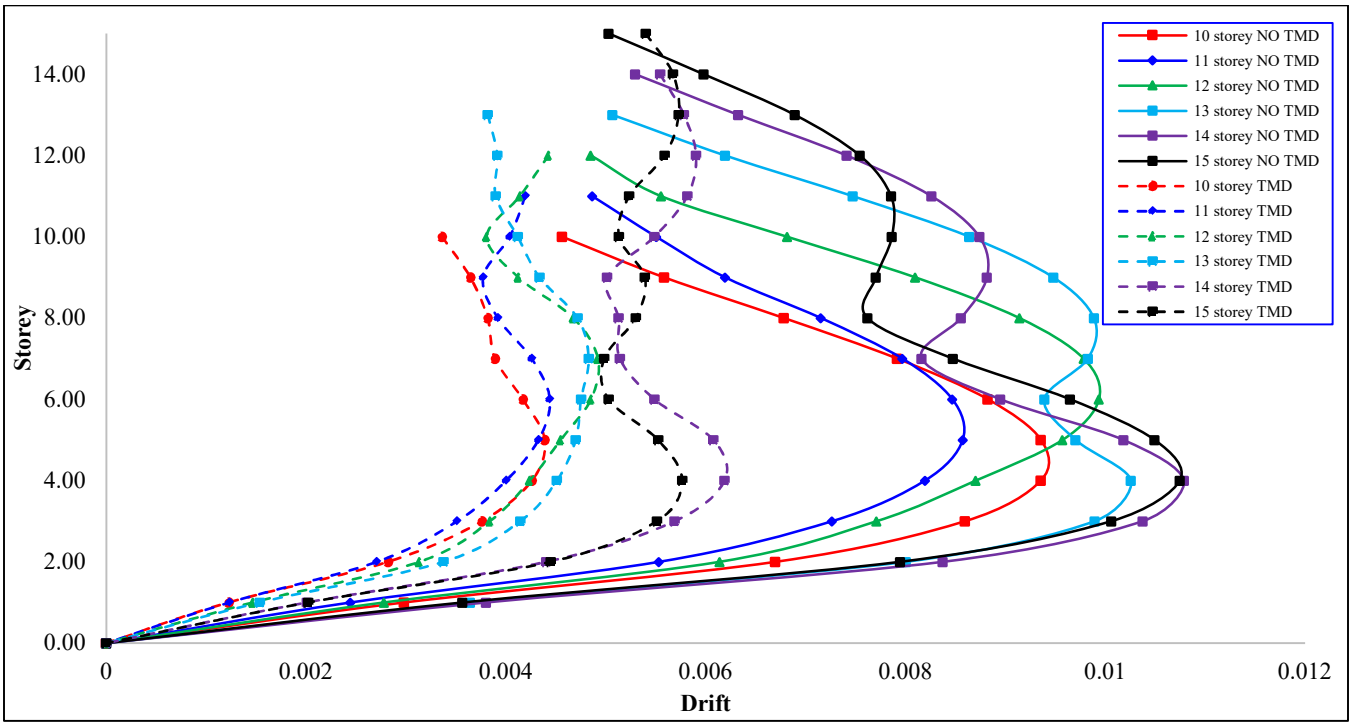

Fig. 20 Drift in structures from 15 to 10 storeys

Figure 20 shows the reduction percentages as follows: buildings with 10 storeys: 53.10%, buildings with 11 storeys: 48.22%, buildings with 12 storeys: 50.48%, buildings with 13 storeys: 52.93%, buildings with 14 storeys: 42.63%, and buildings with 15 storeys: 46.37%. This indicates a slight variation in the efficiency of the devices, with the greatest performance in the lowest buildings and a slight decline in efficiency as the buildings became taller. The disconnected curves corresponding to the strata with dissipators were still lower than the continuous curves without dissipators, which shows a considerable amount of reduction in the lateral drifts and a larger construction with a more controlled and rigid response. The greatest separations between the curves were in the 10, 12, and 13-storey buildings, which were related to the more effective energy dissipation, as were the 14 and 15-storey buildings that showed a smaller response and were therefore less energy dissipating due to the smaller amplitude of the relative displacements. Overall, the figure showed that the incorporation of the viscous-fluid dissipator promoted a homogeneous redistribution of drifts, reduced the concentration of deformations in the upper levels, and improved overall stability under seismic excitations, consolidating its effectiveness as a passive structural control mechanism in medium-rise buildings.

4.2.5. Accelerations in Structures from 20 to 16 Storeys

Table 16 shows that the maximum acceleration decreased progressively when the tuned mass damper (TMD) was incorporated, especially in the taller models, where structural vibrations reached more significant amplitudes. In 16-storey buildings, acceleration decreased from 7.3679 m/s² to 7.0796 m/s², demonstrating slight control of the dynamic response by the TMD, which partially reduced the transmission of inertial energy. On the 17th floor, the value decreased from 7.1229 m/s² to 6.8481 m/s², showing similar behaviour, in which the tuned mass acted as a secondary damper capable of absorbing part of the seismic excitation. On 18 floors, the acceleration was reduced from 7.7796 m/s² to 6.5217 m/s², reflecting a more noticeable improvement in dynamic stability, as the system was close to its optimal tuning frequency. On 19 floors, the value dropped from 7.9628 m/s² to 5.3932 m/s², representing the best performance of the device, as the greater relative displacement allowed the TMD to work more efficiently and counteract lateral accelerations. Finally, on 20 floors, the acceleration decreased from 7.5618 m/s² to 5.6452 m/s², confirming that the system maintained its dissipation capacity in buildings with greater mass and structural period.

Table 3. Accelerations in structures from 20 to 16 storeys

Storey	Without TMD (m/s²)	With TMD (m/s²)	% Reduction
16	7.3679	7.0796	3.913%
17	7.1229	6.8481	3.858%
18	7.7796	6.5217	16.169%
19	7.9628	5.3932	32.270%
20	7.5618	5.6452	25.346%

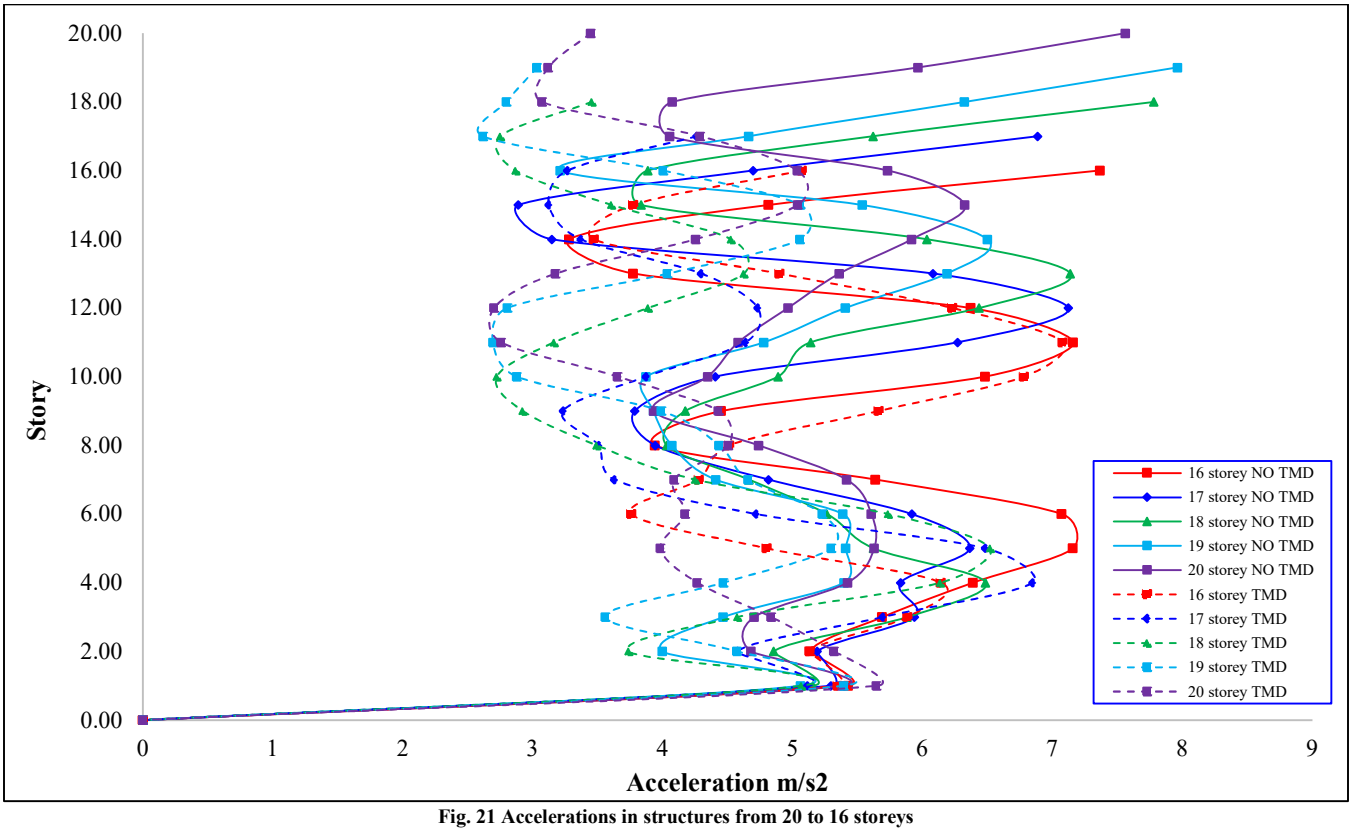

Fig. 21 Accelerations in structures from 20 to 16 storeys

Figure 21 demonstrates that 16 floors had 3.913% reduction in deceleration, 17 floors had 3.858% reduction, 18 floors had 16.169% reduction, 19 floors had 32.270% reduction, and 20 floors had 25.346% reduction, demonstrating that as the building increased in height, the effectiveness of the system increased more and more. The discontinuous curves (structures with TMD) were always below the continuous curves (without TMD), showing a net increase in reduction of acceleration at all height levels, particularly in the taller models. The distance between the curves was greatest when there were 18 and 19 floors, where the device performed the best and (most likely) coincided with the TMD's natural frequency and the building's predominant frequency. For the buildings with 16 and 17 floors, the difference was smaller because as the building was smaller, there was less flex in the structure, which decreased the damper's effectiveness. For the 20-storey building, the increase in the difference was still significant, which means that there was still good control of acceleration at the top of the building.

4.2.6. Accelerations in Structures from 15 to 10 Storeys

Given the tuned mass damper (TMD) capabilities to mitigate vibration, as shown in Table 17, the maximum acceleration dropped in all examples. Within a 10-storey construction, the acceleration dropped to 10.1583 m/s² from 16.9991 m/s², due to out-of-phase interaction where the tuned mass and the primary structure absorbed some of the inertial energy of the system. Out of 11 floors, the acceleration also dropped from 13.2935 m/s² to 9.3797 m/s², indicating that the TMD successfully defeated the resonant oscillation by synchronizing its frequency to the first mode of the structure's primary frequency. On the 12th floor, the acceleration was reduced from 11.3366 m/s² to 9.2323 m/s², showing a more damped response as a result of the increase in energy dissipation. On the 13th floor, the value decreased from 10.0937 m/s² to 7.4827 m/s², indicating a significant reduction in maximum lateral acceleration by improving the balance between stiffness and mass. On 14 floors, the acceleration decreased from 8.3667 m/s² to 7.1283 m/s², maintaining stable behaviour, while on 15 floors, it decreased from 9.299 m/s² to 7.8066 m/s², demonstrating that the system maintained its effectiveness even in models with a longer fundamental period.

Table 17. Aceleraciones en estructuras de 15 a 10 pisos

Storey	Without TMD (m/s^2)	With TMD (m/s^2)	% Reduction
10	16.9991	10.1583	40.242%
11	13.2935	9.3797	29.441%
12	11.3366	9.2323	18.562%
13	10.0937	7.4827	25.868%
14	8.3667	7.1283	14.802%
15	9.299	7.8066	16.049%

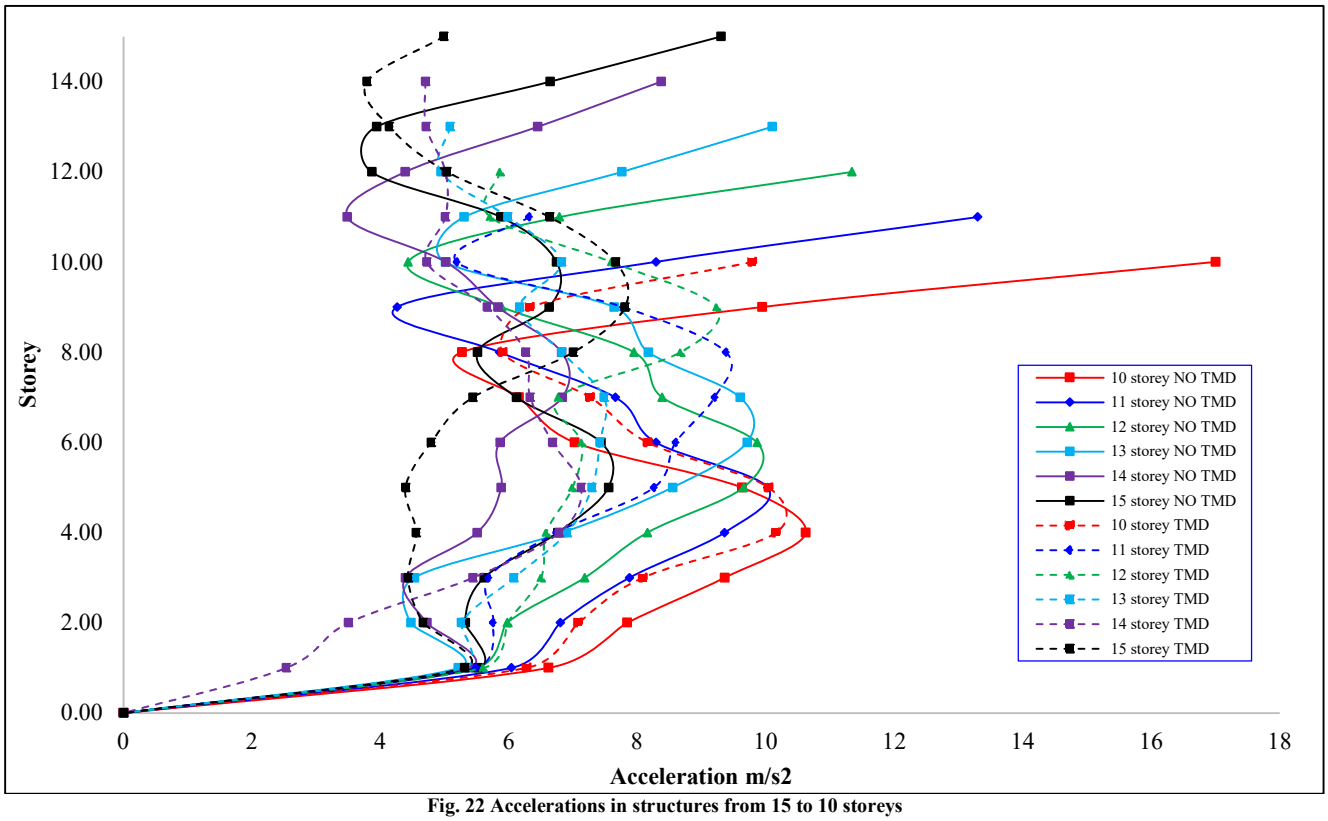

Fig. 22 Accelerations in structures from 15 to 10 storeys

Figure 22 shows that the reduction percentages were 40.242% in buildings with 10 storeys, 29.441% in buildings with 11 storeys, 18.562% in buildings with 12 storeys, 25.868% in buildings with 13 storeys, 14.802% in buildings with 14 storeys, and 16.049% in buildings with 15 storeys, indicating a decreasing trend in TMD efficiency as the building height increased and the distribution of effective modal mass changed. The discontinuous curves corresponding to the buildings with TMD were located below the continuous curves without TMD, indicating an overall reduction in maximum lateral acceleration across all levels. The widest separations between curves were observed in the buildings with 10 and 13 storeys, where the device operated most effectively as its natural frequency aligned with that of the structural system. In the buildings with 11, 12, 14, and 15 storeys, the distance between curves was smaller, reflecting more moderate dissipation associated with the lower relative kinetic energy between the main mass and the tuned mass.

4.2.7. Shear Force at the Base

Table 18 shows that the shear force at the base decreased in all buildings after the implementation of the tuned mass damper (TMD), demonstrating its effectiveness in reducing the seismic demand transmitted to the foundations. On 10 floors, the value went from 2118.18 tonnes to 1676.94 tonnes, indicating a reduction associated with the counterphase effect generated by the relative movement of the TMD, which dissipated part of the input energy. On 11 floors, the force decreased from 2250.77 tonnes to 1424.66 tonnes, demonstrating a considerable reduction in shear forces due to improved modal damping. On 12 floors, the reduction from 2096.63 tonnes to 1480.43 tonnes reflected the device's ability to absorb acceleration peaks, while on the 13th floor, the variation from 2844.27 tonnes to 1339.16 tonnes represented one of the most significant decreases, attributed to more effective tuning between the structural period and that of the TMD. On 14 floors, the force decreased from 3188.76 tonnes to 2287.05 tonnes, showing a moderate reduction, while on 15 floors, the value decreased from 3356.45 tonnes to 1830.01 tonnes, confirming a significant improvement in the baseline seismic response. In the 16- to 20-storey models, the shear forces were reduced steadily: from 3056.67 tonnes to 1709.00 tonnes, from 2892. 81 tonnes to 1,465.92 tonnes, from 2991.77 tonnes to 1232.18 tonnes, from 3037.74 tonnes to 1217.60 tonnes, and from 2799.73 tonnes to 1506.46 tonnes, respectively. Overall, the values demonstrated that the TMD mitigated the shear forces transmitted to the base, stabilising the structure and reducing the risk of load concentrations on the supports, which resulted in more efficient and controlled seismic behaviour.

Table 18. Shear force at the base

Story	Without TMD	With TMD	% Reduction
10	2118.18	1676.94	20.83%
11	2250.77	1424.66	36.70%
12	2096.63	1480.43	29.39%
13	2844.27	1339.16	52.92%
14	3188.76	2287.05	28.28%
15	3356.45	1830.01	45.48%
16	3056.67	1709.00	44.09%
17	2892.81	1465.92	49.33%
18	2991.77	1232.18	58.81%
19	3037.74	1217.60	59.92%
20	2799.73	1506.46	46.19%

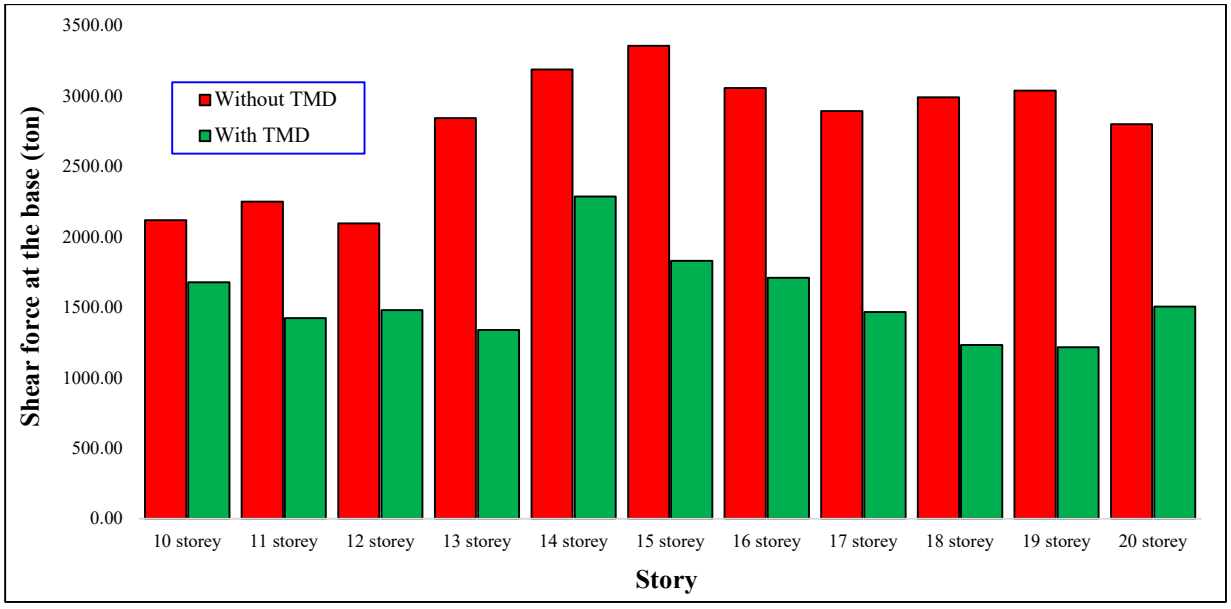

Fig. 23 Shear force at the base

In Figure 23, the reduction percentages ranged from 20.83% to 59.92%, with superior performance in the buildings with 13, 15, 17, 18, and 19 storeys, which achieved reductions of 52.92%, 45.48%, 49.33%, 58.81%, and 59.92%, respectively. The green bars, corresponding to the structures with TMD, were consistently lower than the red bars representing the structures without TMD, showing a clear decrease in the force transmitted to the base in all cases. This difference was most pronounced in the buildings with 18 and 19 storeys, where the device reached maximum efficiency due to the alignment between its oscillation frequency and that of the structural system, allowing for more effective dissipation of seismic energy. In the buildings with 10, 11, 12, and 14 storeys, the reductions were more moderate, although they maintained the downward trend, demonstrating that even in lower-height configurations, the TMD contributed to improving base stability. Overall, the graph showed that the tuned mass system acted as a dynamic decoupling mechanism, reducing the inertial forces generated by the earthquake and promoting a more balanced structural response. This behaviour confirmed that the TMD not only improved the overall damping capacity but also significantly reduced the shear demand at the base, increasing structural safety and prolonging the service life of the resistant system

4.3. Practical Implementation and Structural Implications

From a practical implementation perspective, both control systems present important considerations for real-world applications. In terms of failure modes, the observed reductions in inter-storey drift and displacement suggest a lower probability of structural damage, such as plastic hinge formation, excessive deformation, or instability mechanisms, particularly in buildings with geometric irregularities due to re-entrant corners. Regarding constructability, the Chevron Brace viscous fluid system offers advantages due to its ease of integration into conventional structural frames and its compatibility with typical construction practices. In contrast, the TMD requires additional space at the top of the structure, as well as specialized installation and tuning to match the dynamic properties of the building. From an economic perspective, the viscous fluid system may represent a more cost-effective and modular solution, while the TMD generally involves higher initial costs due to the mass, mechanical components, and installation requirements. Additionally, maintenance considerations must be taken into account, as TMD systems require periodic calibration, whereas viscous dampers tend to have more stable long-term performance. These aspects highlight that, beyond structural efficiency, the selection of the control system must also consider practical feasibility, cost implications, and long-term performance in real structural applications.

5. Discussion

Due to the lack of background data comparing the use of TMDs and viscous fluid dissipators in Chevron Brace arrangements in structures with irregularities due to inward corners, a comparison was made with structures of normal configuration incorporating TMDs and viscous fluid.

According to Shahi's study [35], the implementation of an Active Tuned Mass-Damper Inerter (ATMDI) system controlled by a Tilt Integral Derivative (TID-S) scheme achieved reductions of 61.39% in peak acceleration, 62.70% in RMS acceleration, and up to 35.3% in RMS displacements in a 40-storey building subjected to wind loads. This system, optimized with the Whale Optimization Algorithm (WOA) algorithm, combined tuned mass with an active inverter, significantly reducing the vibrational response without requiring high masses and keeping control forces within practical limits. In addition, it was found that TMDI and ATMDI reduced physical mass by 40.86% and 21.56%, respectively, compared to conventional TMDs, increasing the energy efficiency and adaptability of the structural control system. Similarly, in the present study, both control systems showed a significant capacity to reduce maximum displacements in irregular buildings with 10 to 20 storeys and re-entrant corner irregularities. The most noticeable reductions were observed in the taller models, particularly those with 18 and 19 storeys. In the case of the VFD system, displacement reductions ranged from 17.43% to 59.93%, while the TMD system reached reductions of up to 60.27%. These results indicate that passive control systems can also provide a stable reduction in seismic response in irregular buildings, especially in structures with greater flexibility and higher modal participation, where control is more favorable within the elastic deformation range. The differences between Shahi et al.'s study and the present study are mainly explained by the type of excitation, structural height, and control strategy. Shahi et al. focused on a regular 40-storey building subjected to wind loading and equipped with an active control system, whereas the present study examined mid-rise buildings with re-entrant corner irregularities subjected to seismic excitation and controlled through passive devices. Therefore, although both Shahi et al.'s study and the present study confirm the effectiveness of mass-based damping systems (such as TMDs), the present results also show that passive control strategies, including viscous fluid dampers, can achieve substantial reductions in irregular mid-rise buildings under seismic loading.

Cáceres, Pichihua, and Huaco [36] conducted a study whose objective was to determine the seismic strengthening of a confined masonry hospital structure using diagonally placed Viscous Fluid Dampers (VFDs). Using time-history analysis based on representative records from Lima (1966), Áncash (1970), and Lima (1974), the drift of the structure was reduced from 0.6% to 0.3%, and the service limit for E.030 (Essential Buildings) was satisfied. Efficiency was best on the transverse axis of the structure, where dampers placed on the outermost girders exhibited stable behaviour and did not require the installation of additional shear walls. The authors mentioned that the FVDs alleviated the shear stress on the walls to a level

acceptable by E.070, allowing the walls to function after the earthquake. In the present study, the reduction of inter-storey drift was also significant in buildings with 10 to 20 storeys and re-entrant corner irregularities. In the case of the viscous system, reductions ranged from 16.32% to 56.52%, showing a substantial increase in effective dynamic stiffness and lateral stability. The TMD system, in turn, reduced drifts by up to 53.10%, promoting a more uniform response between storeys and efficient control of the torsional effects generated by geometric irregularity. Both devices made it possible to keep relative displacements within regulatory limits, thereby improving seismic performance without compromising the expected ductile behavior of the structure. The differences between Cáceres' study and the present research lie mainly in the structural typology and geometric distribution of irregularities. Cáceres' research analyzed a regular five-storey confined masonry building, where control was concentrated on the transverse axis, whereas the present research addressed mid-rise reinforced concrete structures with re-entrant corners, where drifts are amplified by the eccentricity between mass and stiffness. Consequently, although both studies confirm the effectiveness of VFDs, the present study extends their application to more complex irregular configurations and additionally allows a direct comparison between VFDs and TMDs under seismic loading.

These comparisons, summarised in Table 19, indicate that although the analysed studies differ in structural typology and excitation type, the reductions achieved in the present study are comparable to those reported in previous research, demonstrating that passive control systems can attain performance levels similar to those of more complex or active control strategies in irregular mid-rise buildings.

Table 4. Structural irregularities in the floor plan

Study	Structural type	Control system	Main response parameter	Maximum reduction	Key observation
Shahi et al. (2025)	Regular 40-storey building	ATMDI (active system)	Acceleration/displacement	Up to 61.39% (peak acc.); 35.3% (disp.)	High efficiency under wind loading using active control
Cáceres et al.	Regular 5-storey confined masonry	VFD	Inter-storey drift	0.6% - 0.3% (50%)	Effective drift reduction in low-rise regular structures
Present study (VFD)	Irregular mid-rise (10-20 storeys)	VFD (Chevron Brace)	Displacement/drift	Up to 59.93% (disp.); 56.52% (drift)	Improves stiffness and lateral stability in irregular structures
Present study (TMD)	Irregular mid-rise (10-20 storeys)	TMD	Displacement/drift	Up to 60.27% (disp.); 53.10% (drift)	Efficient torsional control and uniform response

6. Conclusion

Firstly, the comparative analysis showed that the Tuned Mass Damper (TMD) achieved the greatest overall control in tall buildings, particularly those with 18 and 19 floors, where it achieved displacement reductions of up to 60.27% and reductions in base shear forces of close to 59.92%. This performance is due to its ability to synchronise its frequency with the predominant mode of the structure, generating counterphase oscillations that counteract the dynamic response. Its behaviour became progressively more efficient as structural flexibility increased, confirming its suitability for slender structures or those with long periods, where the resonant action of the system is decisive in controlling global deformations and redistributing stresses.

Secondly, the Chevron Brace viscous fluid dissipator showed more stable, consistent, and predictable behaviour in low and medium-rise buildings (10 to 15 storeys), with displacement reductions of up to 59.93%, maximum accelerations of up to 58.43%, and drifts of up to 56.52%. At higher points in a structure, the relative velocity between levels will be lower, which will yield slight decreases in efficiency. However, the control of local vibrations with the rigid configurations was, in the response, absolutely remarkable and was in the elastic range. This shows that, with abrupt and impulsive motions, the viscous dissipation response is rapid, and in the seismic control of fluids, the energy is transformed to heat with the damping fluid.

Thirdly, from a performance-based design perspective, the two systems demonstrated complementary benefits in basal shear and displacement reductions. The TMD is ideal for overall response control and resonance in high-rise systems, as it reduces basal shear and displacement by up to 60%, effectively controlling global structural response. In contrast, the Chevron Brace system offers better control of instantaneous accelerations and drifts (up to 58% and 56%, respectively), making it more suitable for compact, mid-rise buildings. Therefore, the selection of the optimal system depends directly on the height, stiffness, and type of geometric irregularity of the structure: the viscous fluid responds better to immediate stresses, while the TMD is more efficient in regulating prolonged vibrational response.

Fourthly, analysis of the shear force at the base confirmed the effectiveness of both passive control mechanisms. The Chevron Brace achieved reductions of up to 48.14% in 13-storey structures, showing uniform and sustained behaviour throughout the height, while the TMD obtained values between 20.83% and 59.92%, with the best results in tall buildings of 18 and 19 storeys. This contrast indicates that the viscous system dissipates energy directly at the intermediate levels, reducing the transmission of forces to the base, while the TMD acts by dynamically decoupling the structural mass, decreasing the global inertial forces.

Finally, it is concluded that the Chevron Brace viscous fluid dissipator is the most stable, versatile, and reliable alternative for low- and medium-rise buildings with irregularities due to recessed corners, due to its ability to control accelerations simultaneously and drifts. For its part, the Tuned Mass Damper (TMD) is established as the most efficient in tall structures, where it significantly reduces global displacements and stresses by taking advantage of its resonant effect. From the standpoint of structural performance, both systems improved seismic behaviour by reducing deformation demands, limiting structural and non-structural damage, and enhancing the overall safety of the structure under seismic excitation. Both systems demonstrated complementary performance, contributing to passive seismic control within the elastic range, increasing structural safety, and providing a solid basis for future combined applications (Chevron + TMD) in irregular reinforced concrete structures.

Future research should focus on evaluating the combined implementation of TMD and viscous fluid dampers in irregular structures, as well as exploring their performance under different seismic records and soil conditions. Additionally, further studies are recommended to include probabilistic analyses, cost optimization, and long-term performance assessment in order to enhance the practical applicability of these systems in real engineering projects. Moreover, the potential applicability of these control systems to other types of dynamic hazards, such as wind loads, traffic-induced vibrations, or blast effects, should also be considered as a relevant direction for future research.

Conflicts of Interest

The authors declare that there is no conflict of interest regarding the publication of this article.

References

[1] Geophysical Institute of Peru, gob.pe, 1922. [Online]. Available: https://www.gob.pe/igp

[2] Infobae, Pisco Earthquake 7.9: The Pain, Devastation and Death that Still Remain in the Memory of Peruvians, Infobae, 2022. [Online]. Available: https://www.infobae.com/america/peru/2022/08/15/terremoto-en-pisco-79-el-dolor-devastacion-y-muerte-que-aun-sigue-en-la-memoria-de-los-peruanos/

[3] Ministry of Housing, Construction and Sanitation, Standard E.030: Seismic-Resistant Design, Lima, Peru, 2020. [Online]. Available: https://drive.google.com/file/d/1W14N6JldWPN8wUZSqWZnUphg6C559bi-/view?usp=sharing

[4] Shehata E. Abdel Raheem et al., "Evaluation of Plan Configuration Irregularity Effects on Seismic Response Demands of L-Shaped MRF Buildings," *Bulletin of Earthquake Engineering*, vol. 16, no. 9, pp. 3845-3869, 2018. [CrossRef] [Google Scholar] [Publisher Link]

[5] Shehata E. Abdel Raheem et al., "Seismic Performance of L-Shaped Multi-Storey Buildings with Moment-Resisting Frames," *Proceedings of the Institution of Civil Engineers - Structures and Buildings*, vol. 171, no. 5, pp. 395-408, 2018. [CrossRef] [Google Scholar] [Publisher Link]

[6] Ali Rodríguez-Castellanos et al., "Multi-Disciplinary Performance Comparison for Selecting the Optimal Sustainable Design of Buildings Structures with Fluid-Viscous Dampers," *Soil Dynamics and Earthquake Engineering*, vol. 178, pp. 1-18, 2024. [CrossRef] [Google Scholar] [Publisher Link]

[7] Luyue Yan et al., "Seismic Control of Cross Laminated Timber (CLT) Structure with Shape Memory Alloy-based Semi-Active Tuned Mass Damper (SMA-STMD)," *Structures*, vol. 57, pp. 1-14, 2023. [CrossRef] [Google Scholar] [Publisher Link]

[8] Salah Djerouni et al., "Multi-Tuned Mass Damper Inerter (MTMDI) System for Earthquake-Induced Vibration Control of Buildings," *Engineering Structures*, vol. 322, pp. 1-19, 2025. [CrossRef] [Google Scholar] [Publisher Link]

[9] Shangtao Hu et al., "Theoretical and Numerical Study of the Thermo-Mechanical Coupling Effect on the Fluid Viscous Damper," *Journal of Sound and Vibration*, vol. 597, 2015. [CrossRef] [Google Scholar] [Publisher Link]

[10] TVPerú, Pisco Earthquake, 2007: 17 Years Since a Devastating Earthquake, 2024. [Online]. Available: https://www.tvperu.gob.pe/noticias/nacionales/terremoto-en-pisco-2007-17-anos-de-un-sismo-devastador

[11] El Búho, It's Been 20 Years Since the 8.4 Magnitude Earthquake that Shook Arequipa, 2021. [Online]. Available: https://elbuho.pe/2021/06/se-cumplen-20-anos-del-terremoto-de-8-4-de-magnitud-que-sacudio-arequipa/

[12] Infobae, Earthquake in Peru: What have been the Deadliest and Most Destructive Earthquakes in Recent Years?, 2023. [Online]. Available: https://www.infobae.com/peru/2023/12/20/temblor-en-peru-cuales-han-sido-los-sismos-mas-mortales-y-destructivos-de-los-ultimos-anos/

[13] Geophysical Institute of Peru: IGP will Hold a Virtual Conference "1974 Earthquake: The Earthquake that Changed the Face of Lima and Callao," 2021. [Online]. Available: https://www.gob.pe/institucion/igp/noticias/305060-igp-realizara-conferencia-virtual-terremoto-de-1974-el-sismo-que-cambio-el-rostro-de-lima-y-el-callao

[14] Jitendra Gudainiyan, and Praveen Kumar Gupta, "Parametric Study of L-Shaped Irregular Building Under Near-Field Ground Motion," *Asian Journal of Civil Engineering*, vol. 24, no. 7, pp. 2561-2570, 2023. [CrossRef] [Google Scholar] [Publisher Link]

[15] Reyes Indira Herrera González, Andrés Alejandro Ramírez Pírela, and Ronald David Ugel Garrido, "Study of Seismic Response and Global Damage of Two Irregular Buildings of Reinforced Concrete," *Saber*, vol. 28, no. 2, pp. 279-292, 2016. [Google Scholar] [Publisher Link]

[16] I. A. Villafuerte Lujano and V. I. Fernández-Dávila Gonzales, "Seismic response of 8-story reinforced concrete buildings with irregular floor plan," *Ingeniería*, vol. 34, no. 2, pp. 21–37, 2024. [CrossRef] [Google Scholar] [Publisher Link]

[17] Luigi Petti, and Massimiliano De Iuliis, "Torsional Seismic Response Control of Asymmetric-Plan Systems by using Viscous Dampers," *Engineering Structures*, vol. 30, no. 11, pp. 3377-3388, 2008. [CrossRef] [Google Scholar] [Publisher Link]

[18] Bharat Khanal, and Hemchandra Chaulagain, "Seismic Elastic Performance of L-Shaped Building Frames Through Plan Irregularities," *Structures*, vol. 27, pp. 22-36, 2020. [CrossRef] [Google Scholar] [Publisher Link]

[19] Momen M.M. Ahmed et al., "Irregularity Effects on the Seismic Performance of L-Shaped Multi-Story Buildings," *Journal of Engineering Sciences Assiut University Faculty of Engineering*, vol. 44, no. 5, pp. 513-536, 2016. [Google Scholar]

[20] Avadhoot S. Bhosale, Robin Davis, and Pradip Sarkar, "Seismic Safety of Vertically Irregular Buildings: Performance of Existing Indicators," *Journal of Architectural Engineering*, vol. 24, no. 3, 2018. [CrossRef] [Google Scholar] [Publisher Link]

[21] Pranab Kumar Das, Sekhar Chandra Dutta, and Tushar Kumar Datta, "Seismic Behavior of Plan and Vertically Irregular Structures: State of Art and Future Challenges," *Natural Hazards Review*, vol. 22, no. 2, 2021. [CrossRef] [Google Scholar] [Publisher Link]

[22] Mohamed Sherif Mehana, Osama Mohamed, and Feda Isam, "Torsional Behaviour of Irregular Buildings with Single Eccentricity," *IOP Conference Series: Materials Science and Engineering*, vol. 603, no. 5, pp. 1-10, 2019. [CrossRef] [Google Scholar] [Publisher Link]

[23] Ghazal Gholami, Hossein Abadi, and Hesam Varaee, "Effect of Torsional Irregularity on Seismic Performance of Steel Moment Resisting Frame Structures," *Advance Researches in Civil Engineering*, vol. 5, no. 1, pp. 1-30, 2023. [Google Scholar]

[24] Zhihua Chen et al., "Exploration of the Multidirectional Stability and Response of Prefabricated Volumetric Modular Steel Structures," *Journal of Constructional Steel Research*, vol. 184, 2021. [CrossRef] [Google Scholar] [Publisher Link]

[25] Livian Teddy et al., "The Effect of Earthquake on Architecture Geometry with Non-Parallel System Irregularity Configuration," *IOP Conference Series: Earth and Environmental Science*, vol. 99, no. 1, pp. 1-7, 2017. [CrossRef] [Google Scholar] [Publisher Link]

[26] Ministry of Housing, Construction and Sanitation: National Building Regulations - RNE, 2021. [Online]. Available: https://www.gob.pe/institucion/vivienda/informes-publicaciones/2309793-reglamento-nacional-de-edificaciones-rne

[27] Kul Vaibhav Sharma et al., "Modelling Efficiency of Fluid Viscous Dampers Positioning for Increasing Tall Buildings' Resilience to Earthquakes-Induced Structural Vibrations," *Soil Dynamics and Earthquake Engineering*, vol. 173, 2023. [CrossRef] [Google Scholar] [Publisher Link]

[28] Ahmed Sabah Aljawadi, Mohammadreza Vafaei, and Sophia C. Alih, "Seismic Strengthening of Deficient Ground Soft-Story RC Frames with Inadequate Lap Splice using Chevron Brace," *Structures*, vol. 61, 2024. [CrossRef] [Google Scholar] [Publisher Link]

[29] Olivier Gauron et al., "Design and Performance of Autonomous Chevron-Brace Systems with Elastomeric-Dampers for Steel Frames," *Journal of Constructional Steel Research*, vol. 115, pp. 34-46, 2015. [CrossRef] [Google Scholar] [Publisher Link]

[30] Building Officials and Code Administrators International. [Online]. Available: https://www.encyclopedia.com/law/encyclopedias-almanacs-transcripts-and-maps/building-officials-and-code-administrators-international

[31] Chavez Chavarria et al., "*Seismic Analysis of Block a of the Luis Negreiros Hospital with and Without Viscous Fluid Energy Dissipator Protection*," Thesis, Peruvian University of Applied Sciences (UPC), Lima, Perú, 2020. [Google Scholar] [Publisher Link]

[32] Qi Wang, Hong-Nan Li, and Peng Zhang, "Vibration Control of a High-Rise Slender Structure with a Spring Pendulum Pounding Tuned Mass Damper," *Actuators*, vol. 10, no. 3, pp. 1-19, 2021. [CrossRef] [Google Scholar] [Publisher Link]

[33] Hosein Naderpour et al., "Optimizing Seismic Performance of Tuned Mass Dampers at Various Levels in Reinforced Concrete Buildings," *Buildings*, vol. 14, no. 8, pp. 1-19, 2024. [CrossRef] [Google Scholar] [Publisher Link]

[34] Mohammad Jafari, and Alice Alipour, "Methodologies to Mitigate Wind-Induced Vibration of Tall Buildings: A State-of-the-Art Review," *Journal of Building Engineering*, vol. 33, pp. 1-60, 2021. [CrossRef] [Google Scholar] [Publisher Link]

[35] Agathoklis Giaralis, and Francesco Petrini, "Wind-Induced Vibration Mitigation in Tall Buildings using the Tuned Mass-Damper-Inerter," *Journal of Structural Engineering*, vol. 143, no. 9, pp. 1-29, 2017. [CrossRef] [Google Scholar] [Publisher Link]

[36] Gladys Cáceres-Pérez, Natali Pichihua-Alata, and Guillermo Huaco-Cárdenas, "Seismic Retrofit in Hospitals using Fluid Viscous Dampers," *2020 International Congress on Innovation and Trends in Engineering (CONIITI)*, Bogota, Colombia, pp. 1-6, 2020. [CrossRef] [Google Scholar] [Publisher Link]